Efficient derivation of neural precursors and dopamine neurons from human embryonic stem cells and their application to a Parkinsonian rat model

Ji-Yun Ko

Department of Medical Science
The Graduate School, Yonsei University

Efficient derivation of neural precursors and dopamine neurons from human embryonic stem cells and their application to a Parkinsonian rat model

Ji-Yun Ko

Department of Medical Science
The Graduate School, Yonsei University

Efficient derivation of neural precursors and dopamine neurons from human embryonic stem cells and their application to a Parkinsonian rat model

Directed by Professor Dong-Wook Kim

The Doctoral Dissertation
submitted to the Department of Medical Science
the Graduate School of Yonsei University
in partial fulfillment of the requirements for the degree of
Doctor of Philosophy of Medical Science

Ji-Yun Ko

June 2010

This certifies that the Doctoral Dissertation of Ji-Yun Ko is approved

---

Thesis Supervisor : Dong-Wook Kim

Thesis Committee Member : Phil Hyu Lee

Thesis Committee Member : Hyun Ok Kim

Thesis Committee Member : Sang-Hun Lee

Thesis Committee Member : Chang-Hwan Park

The Graduate School

Yonsei University

June 2010

ACKNOWLEDGEMENTS

여러 이유로 중단되었던 학업을 다시 시작하려고 하였을 때, 걱정스럽게 바라보던 많은 시선들이 생각납니다. 잘 해낼 수 있을지 스스로도 많이 의문스럽던 시간들이었음에도 끝까지 포기하지 않고 지금 이 순간을 맞이할 수 있었던 건, 저 혼자만의 노력이 아니었음을 잘 알고 있습니다. 힘들었던 순간 순간마다 다시 일어설 수 있도록 도움과 격려를 아끼지 않으셨던 많은 고마운 분들이 아니었다면 지금 이 시간 또한 저에게 허락되지 않았을 시간임을 잘 압니다.

논문 지도를 해주신 교수님들께 깊은 감사의 마음을 전합니다. 바쁘신 중에도 여러 가지로 신경써 주시고 좋은 논문이 되도록 지도해주신 김동욱 교수님의 따뜻한 은혜에 진심으로 감사드립니다. 저에게 힘든 일이 있을 때마다 말없이 걱정하고 조용히 기도해주셨을 이상훈 교수님께도 감사드립니다. 많은 것이 부족했던 저에게 그나마 지금의 순간이 있을 수 있었던 건 모두 교수님의 배려와 격려 덕분이었음을 항상 잊지 않겠습니다. 사람 배아줄기세포 배양을 꼼꼼하게 가르쳐주시고 어려운 문제가 생길 때마다 자신의 일처럼 도와주셨던 박장환 교수님께도 이 지면을 빌어 감사의 마음을 전합니다. 또한 좋은 논문이 되도록 바쁘신 중에도 시간내어 자문해주신 김현옥 교수님과 이필휴 교수님께도 진심으로 감사드립니다.
여러 해 동안 실험실에서 함께 생활하며 크고 작게 저에게 도움을 주었던 모든 실험실 식구들에게도 고마운 마음을 전합니다. 또한, 여러모로 신경써주시고 도와주셨던 김대성 박사님께도 감사드립니다.

아이 때문에 선뜻 결정을 내리지 못하고 망설이고 있을 때, 아빠와 떨어져 지내셔야 함에도 아이를 돌봐주시기로 어려운 결정을 해주신 엄마가 아니셨다면 엄두도 못내었을 일이었습니다. 엄마 손이 한참 필요할 시기의 아이에게 엄마의 빈자리를 채워주신 친정 엄마, 저 때문에 본의 아니게 주말 부부로 혼자 생활하신 친정 아빠께 진심으로 머리 숙여 감사드립니다. 제 능력으로는 감당할 수 없었던 학비와 경제적 지원을 아끼지 않고 해주신

시부모님께도 깊이 감사드립니다. 한없이 부족한 며느리에게 늘 따뜻하게 대해주시고 많은 격려와 지원을 아끼지 않으시는 아버님, 너의 일이 우선이라며 다른 것은 신경쓰지 않을 수 있도록 마음 편히 해주시고 도와주신 이해심 많으신 어머님, 진심으로 감사드립니다. 항상 나의 편이 되어주고 든든하게 옆자릴 지켜준 남편에게도 고마운 마음을 전합니다. 바쁘고 힘든 실험실 생활을 오랫동안 지켜보며 함께 힘들어하고, 안쓰러워해준 남편이 있었기에 지금이 있었다고 생각합니다. 감사합니다.

마지막으로, 첫돌 지난 어린 아기일때부터 떼어놓고 나와 올해 학교에 입학한 하나뿐인 나의 소중한 보물 치용이에게 부족하지만 소중한 이 논문을 바치고 싶습니다. 아이와 함께 밥먹고, 잠자고, 유치원가고, 놀이동산에서 공원에서 즐겁게 보냈어야 할 시간들을 대신한 시간 위에 쓰여진 논문이기에 아이에게는 한없이 미안한 마음 뿐입니다. 아이에게 부끄럽지 않은 엄마가 되기 위해 나의 일이 아무리 힘들어도, 아이가 엄마를 떨어져 힘들어하는 것을 알면서도, 중간에 포기할 수 없었던 엄마의 마음을 치용이가 자라면서 이 논문을 보며 이해해 주리라 믿습니다.

앞으로 또 어떤 시간들이 저에게 펼쳐질지 모르지만 늘 다시 새롭게 시작한다는 각오와 겸손한 마음으로 또 다른 목표를 향해 나아가겠습니다. 저에게 가장 소중한 지금 이 시간들을 함께 해주신 모든 분들께 다시 한 번 감사의 마음을 전합니다.

2010 년 6 월

고 지 윤

TABLE OF CONTENTS

LIST OF FIGURES

LIST OF TABLE

Efficient derivation of neural precursors and dopamine neurons from human embryonic stem cells and their application to a Parkinsonian rat model

Ji-Yun Ko

Department of Medical Science

The Graduate School, Yonsei University

(Directed by Professor Dong-Wook Kim)

Human embryonic stem (hES) cells can be guided to differentiate into ventral midbrain-type neural precursor (NP) cells that subsequently generate high yields of dopamine (DA) neurons. These findings indicate that hES-derived NP cells can be a prospective cell source to be used in cell replacement strategies for Parkinson's disease (PD). To further clarify the prospect, we have scrutinized the properties of hES-NP cells in the points of (1) capability of these cells in stably providing human DA neurons in a large scale (2) cell survival and tumorigenic potentials which are the most critical issues for an effective and safe cell therapy.

First, we investigated the potential of hES-NP cells for the large-scale generation of human DA neurons for functional analyses and therapeutic applications. To address this,

hES-NP cells were expanded *in vitro* for 1.5 months with 6 passages, and their proliferation and differentiation properties determined over the NP passages. Interestingly, the total hES-NP cell number was increased by $>2\times10^4$-folds over the *in vitro* period without alteration of phenotypic gene expression. They also sustained their differentiation capacity towards neuronal cells, exhibiting *in vitro* presynaptic DA neuronal functionality. Furthermore, the hES-NP cells can be cryopreserved without losing their proliferative and developmental potential. Taken together, these findings indicate that hES-NP cell expansion is exploitable for a large-scale generation of experimental and transplantable DA neurons of human-origin.

In second part of this thesis, we describe cell survival and tumorigenic aspects of these hES-NP cells that are critical issues in cell therapeutic approaches for PD. Neuroepithelial rosettes, a potentially tumorigenic structure, disappeared during hES-NP cell expansion *in vitro*. Although a minor population of cells positive for Oct3/4, a marker specific for undifferentiated hES cells, persisted in culture during hES-NP cell expansion, they could be completely eliminated by subculturing hES-NPs under differentiation-inducing conditions. Consistently, no tumors/teratomas formed in rats grafted with multi-passaged hES-NPs. However, extensively expanded hES-NP cells easily underwent cell death during differentiation *in vitro* and after transplantation *in vivo*. Transgenic expression of Bcl-XL and sonic hedgehog (SHH) completely overcame the cell survival problems without increasing tumor formation. These findings indicate that hES-NP cell expansion in conjunction with Bcl-XL+SHH transgene expression may provide a renewable and safe source of DA neurons for transplantation in PD.

In conclusion, we provide evidences for hES-NP cells as a continuous, stable, and on-demand source for human DA neurons. Multiple passaging of these NP cells helped for a large scale generation of human DA neuron free from tumor formation potentials. However, survival of the multi-passaged hES-NP cells was drastically decreased *in vitro* and *in vivo* after transplantation. Although transgene expression of Bcl-XL+SHH overcome the cell survival problem, the cell survival issue remain to be further studied.

Key words: Human Embryonic Stem (hES) cells, Neural precursor (NP) cell, Dopamine (DA) neurons, Parkinson's disease (PD), Bcl-XL, Sonic hedgehog (SHH)

Efficient derivation of neural precursors and dopamine neurons from human embryonic stem cells and their application to a Parkinsonian rat model

Ji-Yun Ko

Department of Medical Science

The Graduate School, Yonsei University

(Directed by Professor Dong-Wook Kim)

I. INTRODUCTION

Parkinson's disease (PD) is a common neurodegenerative disorder characterized by loss of dopamine (DA) neurons in the substantia nigra of the midbrain. Given the well-defined neuronal type and locus affected in PD, a cell-transplantation approach offers great promise for the treatment of PD. Human fetal midbrain tissues have been clinically used as a source of DA neurons for transplantation in PD patients. However, this supply is limited and difficult to develop as a routine systematized source. Furthermore, the clinical benefits of fetal nigral transplantation in PD patients are controversial.[1,2] Stem cells with self-renewal capacity and multi-developmental plasticity are regarded as an alternative and attractive source of cells for replacement strategies, not only because they

are capable of yielding consistently functional DA neurons on a large-scale, but also for their potential to provide clear behavioral recovery in PD patients upon transplantation.[3]

Human embryonic stem (hES) cells, derived from the inner cell mass of pre-implanted blastocysts, are multipotent cells, which have the capacity to differentiate into most cell types from the three germ layers. They are expandable *in vitro* and their multipotency can be retained even after multiple passages.[4-6] These properties of hES cells are thought to offer promise of an unlimited source of many cell types, which could be used in basic and translational studies of cell replacement strategies. However, the potential applications of undifferentiated hES cells (especially for the purpose of therapeutic transplantation) are largely hampered by their genomic instability characterized by the high frequency of chromosomal anomalies during *in vitro* culture.[7-9] Furthermore, *in vitro* maintenance and expansion of undifferentiated hES cells is fastidious requiring stringent experimental conditions. In addition, we herein additionally demonstrate the loss of developmental potential of hES cells towards neuronal progeny after maintenance in long-term culture.

Recent studies successfully derived midbrain-type DA neurons from hES cells. These findings support the idea of using hES cells as a renewable source of human DA cells for experimental or therapeutic purposes in PD, a disease characterized by the selective loss of midbrain DA neurons. In contrast to the direct differentiation of hES cells into DA neurons,[10-12] we and Perrier et al. have presented protocols sequentially differentiating hES cells towards DA cells through the intermediary stage of embryonic midbrain-type neural precursor (NP) cells. NP cells derived from hES cells (hES-NP) proliferate *in vitro* with specific mitogen supplementation and differentiate into DA neurons which function *in vitro* as mature presynaptic DA neurons.[13-14] These findings prompted us to test if the

proliferative and DA neurogenic potentials are maintained after prolonged NP expansion *in vitro*, thus supporting the idea of exploiting NP cell proliferation (instead of the problematic expansion of undifferentiated ES cells) for large-scale generation of functional human DA neurons. Therefore, we expanded hES-NP cells *in vitro* for 1.5 months over 6 cell passages, and assessed their developmental properties, survival, and functions *in vitro* and *in vivo* through the improvement of motor dysfunction upon transplantation in rat model of PD.

We assessed cell survival and tumorigenic potential of our hES-NP cells, in order to provide improved donor cell preparation for generating tumor-free graft enriched with DA neurons after transplantation in the present study. Especially we pursued if these two critical aspects of the hES-NP cells could be altered by extended NP cell expansion with multiple passages and in *in vitro* conditions that mimic the *in vivo* environment of the transplant by elimination trophic factors supplemented in culture for cell proliferation and differentiation.

II. MATERIALS & METHODS

1. Culture and differentiation of hES cells

Undifferentiated hES cell lines, HSF-6 (established at University of California, San Francisco, CA, USA; passages 53–82) and H9 (WiCell, Madison, WI, USA; passages 35–38), were grown on γ-irradiated mouse (CF1) embryonic fibroblasts in ES-medium.[13] To induce neural differentiation, hES colonies were transferred onto a feeder layer of γ-irradiated PA6 or MS5 stromal cells and cultured in insulin/transferrin/selenium (ITS) medium[15] with 0.2 mmol/L ascorbic acid (AA) (Sigma, St Louis, MO, USA). Cultures were passaged onto freshly prepared γ-irradiated PA6 or MS5 feeder cells every 7 days, which continued for a total of three to eight passages until a desirable level of neural induction (> 85% hES colonies are differentiated colony with primitive neural structures; hES-NP colonies, see Results) was achieved. For the final round of subculturing, hES colonies were co-cultured on c-irradiated PA6 or MA5 cells stably over-expressing sonic hedgehog (SHH) (PA6-SHH or MS5-SHH).[13] At the end of the co-culture, hES-NP colonies were harvested from the stromal feeder, gently triturated by pipetting into clusters of 50–500 cells in ITS + AA supplemented with basic fibroblast growth factor (bFGF) (20 ng/mL; R&D Systems, Minneopolis, MN, USA), and replated onto poly L-ornithine (PLO) (15 μg/ml, Sigma)/fibronectin (FN) (1 μg/ml, Sigma)-coated culture dishes. After culture for 7–9 days, hES-NP clusters were dissociated into single cells after exposure to Ca2+/Mg2+-free Hank's balanced salt solution for 1 h at 37°C. These were then replated at 2.5 x 10^5 cells/cm2 in ITS + AA + bFGF (NP passage 1, NP-P1). Cells were passaged every 7 days for 42 days (six passages) in medium supplemented with

bFGF. For phenotypic determinations, hES-NP cells were plated on FN-coated glass coverslips (12-mm diameter; Bellco, Vineland, NJ, USA). Terminal differentiation of hES-NP cells was induced in the absence of bFGF but in the presence of brain-derived neurotrophic factor (BDNF) (20 ng/mL; R&D Systems), glial cell linederived neurotrophic factor (GDNF) (20 ng/mL; R&D Systems), dibutyryl cyclic adenosine monophosphate (cAMP) (0.5 mmol/L; Sigma).

2. Population doubling level

The population doubling level (PDL) of hES-NP cells at each NP passage was measured. The formula used for the calculation of population doubling in a single passage is: PDL = log(N/No)/log2, where N is the number of cells in the plate at the end of a period of growth and No is the number of cells plated in the plate (2.5 x 10^5 cells/cm2). Cumulative (total) PDL is total PDL (tPDL) = P(PDL)n, where n is the hES-NP passage number.

3. Retroviral transduction

The retroviral vectors expressing LacZ (control), Bcl-XL, and SHH were constructed as described previously.[16] The bicistronic vector pSHH-IRES-Bcl-XL, designed for the simultaneous expression of SHH and Bcl-XL in the transduced cells, was constructed by replacing LacZ of pSHH-IRES-LacZ with the Bcl-XL complementary DNA fragment amplified by PCR. The retroviral vectors were introduced into the retrovirus packaging cell line 293gpg by transient transfection with Lipofectamine (Invitrogen, Grand Island, NY, USA). After 72 hours, the supernatants were harvested.

The cells were exposed to viral supernatant for 2 hours in the presence of polybrene (1 μg/ml; Sigma).

4. Immunofluorescent staining

Cultured cells and cryosectioned brain slices were fixed in freshly prepared 4% paraformaldehyde in phosphate buffered saline (PBS), and blocked with 5% normal goat serum (NGS) and 0.1% Triton X-100 in PBS at room temperature for 1 hr. In case of detecting human TH+ neurons in transplanted striatum, different antigen retrieval procedures, such as sodium dodecyl sulfate (SDS) treatment or boiling, were employed before the blocking procedure as follows. Sectioned brain slices were treated with 1% SDS in PBS at room temperature (RT) for 5 min and then immersed in PBS.[17-19] For antigen retrieval by boiling, slices were immersed in 10 mM citrate buffer, pH 6.0, and boiled for 15 min in a microwave oven, then chilled on ice for 30 min.[20-22] The following primary antibodies were used: nestin #130 (1:100, Dr. Martha Marvin and Dr. Ron McKay, National Institute of Heath, Bethesda, MD); tyrosine hydroxylase (TH) (1:250, Pel-Freez, Rogers, AR; 1:200, Immunostar, Hudson, WI; 1:1000, Sigma); cleaved Caspase-3 (1:100, Cell Signaling Technology, Beverly, MA); green fluorescence protein (GFP) (1:2000, Invitrogen); glial fibrillary acidic protein (GFAP) (1:100, ICN Biochemicals, Aurora, OH); CNPase (1:500, Sigma); O4 (1:100, Chemicon, Temecular, CA); Nurr1 (NR4A2) (1:100, Santa Cruz Biotechnology, Santa Cruz, CA); human neural cell adhesion molecule (hNCAM) (1:100, Santa Cruz Biotechnology); G protein-gated inwardly rectifying K+ channel (Girk2) (1:200, Sigma; 1:100, Alomone Labs, Jerusalem, Israel); doublecortin (DCX) (1:500, kindly gifted from Dr. Woong Sun, Korea University, Seoul, Korea); Pax2 (1:100, Covance, Richmond, CA); vesicular monoamine transporter

2 (VMAT2) (1:500, Pel-Freez); human nuclei antigen (HN) (1:100, Chemicon); Ki67 (1:100, Novocastra, Newcastle, UK); proliferating cell nuclear antigen (PCNA) (1:40, Upstate biotechnology, Lake Placid, NY); phosphor-Histone H3 (pHH3) (1:100, Upstate cell-signaling solutions, Temecula, CA); Engrailed-1 (En1) (1:50, Developmental Studies Hybridoma Bank, Iowa City, IA); Pax5 (1:50, BD Biosciences, Franklin Lakes, NJ); synapsin (1:1,000, BD Biosciences); neuron-specific class III beta-tubulin (TuJ1) (1:500, Covance); microtubule associated protein 2 (MAP2) (1:200, Sigma); Serotonin (1:4000, Sigma); γ-aminobutyric acid (GABA) (1:700, Sigma); calbindin-D28K (calbindin) (1:250, Chemicon); HuC/D (1:100, Chemicon) and Oct3/4 (1:100, Santa Cruz Biotechnology). Appropriate fluorescence-tagged secondary antibodies (Jackson Immunoresearch Laboratories, West Grove, PA) were used for visualization. Cells and tissue sections were mounted in VECTASHIELD® containing 4',6 diamidino-2-phenylindole (DAPI; Vector Laboratories INC., Burlingame, CA) and analyzed under an epifluorescence microscope (Nikon, Tokyo, Japan) or confocal (Leica PCS SP5, Leica Microsystems Heidelberg GmbH, Heidelberg, Germany) microscope. For LeX immunostaing, live cells were incubated with a LeX antibody (clone MMA, CD15, 1:200, anti-mouse, BD Biosciences), and visualized with a Cy3-conjugated secondary antibody. Coverslips were fixed and mounted for microscopic examination.

5. Propidium iodide staining and lactate dehydrogenase assay

Cultured cells on glass coverslips were stained with propidium iodide (PI) (50 μg/ml, Roche Diagnostics, Germany), fixed in freshly prepared 4% paraformaldehyde in PBS, and mounted in VECTASHIELD® containing DAPI. lactate dehydrogenase (LDH) activity was measured with a Cytotox 96 nonradioactive cytotoxicity assay kit (Promega,

Madison, WI, USA) according to the manufacturer's instructions. Results were expressed as a percentage of maximum LDH release obtained on complete cell lysis following 1.0% Triton X-100 treatment. Fresh ITS medium was used as the negative control (0%).

6. In vivo transplantation and histological procedure

Animals were housed and treated in accordance with guidelines from the National Institutes of Health. Female Sprague-Dawley rats (200-250 g) were lesioned by unilateral stereotactic injection of 6-hydroxydopamine (6-OHDA; Sigma) into the substantia nigra and the median forebrain bundle as described previously.[13] Four weeks later, the animals were tested for drug-induced rotational asymmetry (amphetamine 3 mg/kg i.p., Sigma). Rotation scores were monitored for 60 minutes in an automated rotameter system (Med Associate Inc., St. Albans, Vermont). Animals with ≥ 5 turns/minute ipsilateral to the lesion were selected for transplantation. For transplantation, hES-NP cells expanded with bFGF were harvested and dissociated into single cells. Three microliters of cell suspension (2.5×10^5 cells/μl in PBS) per site were deposited at two sites of the striatum (coordinates in AP, ML, and V relative to bregma and dura: (1) 0.07, -0.30, 0.55; (2) -0.10, -0.40, -0.50; incisor bar set at 3.5 mm using a 22-gauge needle. The needle was left in place for 5 min following each injection. Control sham-operated rats were injected with a vehicle (PBS). The rats received daily injections of cyclosporin A (10 mg/kg, i.p.) starting 24 hours prior to grafting and continuing for 3 weeks, followed by a reduced dose (5 mg/kg) for the remaining time. At 2, 4, 6, and 8 weeks after transplantation, amphetamine-induced rotations were determined. Eight weeks after transplantation, the animals were anesthetized with phenobarbital and perfused transcardially with 4% paraformaldehyde in PBS. Brains were equilibrated with 30% sucrose in PBS and sliced

on a freezing microtome (CM 1850, Leica, Wetzlar, Germany). Free-floating brain sections (35 μm thick) were subjected to immunohistochemistry as described above. TH-immunoreactive cells in the graft were counted by analyzing every sixth uniform section (35 μm thick) with Abercrombie correction.[23] The total number of TH-immunoreactive cells in the graft was estimated by multiplying the sum of TH+ cell counts by six. Graft areas were determined using an image analyzer (Analysis version 3.2, Soft Imaging System, Munster, Germany), and the Cavalieri estimator was used to calculate graft volumes. Hematoxylin and eosin (H&E) staining was carried out with conventional method.

7. Semiquantitative RT-PCR analysis

Total cellular RNA was isolated using TRI REAGENT (Molecular Research Center, Inc. Cincinnati, OH, USA) and cDNA was synthesized from 5 μg of total RNA in a 20 μL reaction using the Superscript kit (Invitrogen). Optimal PCR conditions for each primer set were determined by varying $MgCl_2$ concentrations and annealing temperatures and cycle numbers to determine linear amplification range. Primer sequences, cycle numbers and annealing temperatures were provided in Table 1.

8. Dopamine uptake assay

DA uptake assays were conducted as described previously.[13] Cells were washed with PBS and incubated with 50 nM [^{3}H]DA in PBS (51 Ci/mmol, Amersham Co., Buckinghamshire, UK) with or without 10 μM nomifensine (RBI, Natick, MA), a DAT

Table 1. Information of RT-PCR primer.

Genes	Pimer sequence (F: forward, R: reverse)	Annealing temperatures, Number of PCR cycles, Product sizes (bp)
G3PDH	F: 5' GCTCAGACACCATGGGGAAGGT 3' R: 5' GTGGTGCAGGAGGCATTGCTGA 3'	55℃, 35 cycles, 474 bp
Nestin	F: 5' CAGCGTTGGAACAGAGGT 3' R: 5' TGGCACAGGTGTCTCAAGGGTAC 3'	61℃, 35cycles, 389 bp
Sox1	F: 5' CACAACTCGGAGATCAGCAA 3' R: 5' GTCCTTCTTGAGCAGCAGCGTCT 3'	58℃, 35cycles, 171 bp
Pax6	F: 5' CCAAAGTGGTGGACAAGATTGCC 3' R: 5' TAACTCCGCCCATTCACTGACG 3'	58℃, 35cycles, 419 bp
En1	F: 5' GCAACCCGGCTATCCTACTTATG 3' R: 5' ATGTAGCGGTTTGCCTGGAAC 3'	60℃, 35 cycles, 247 bp
Pax5	F: 5' ATGCAACTGATGGAGTATGAGGAGCC 3' R: 5' CAGATGTAGTCCGCCAAAGGATAG 3'	57℃, 30cycles, 451bp
Lmx 1b	F: 5' ACGAGGAGTGTTTGCAGTGCG 3' R: 5' CCCTCCTTGAGCACGAATTCG 3'	60℃, 30 cycles, 253 bp
Nurr1	F: 5' TTCTCCTTTAAGCAATCGCCC 3' R: 5' AAGCCTTTGCAGCCCTCACAG 3'	60℃, 35 cycles, 332 bp
TH	F: 5' GAGTACACCGCCGAGGAGATTG 3' R: 5' GCGGATATACTGGGTGCACTGG 3'	62℃, 35 cycles, 279 bp
DAT	F: 5' AGCAGAACGGAGTGCAGCT 3' R: 5' GTATGCTCTGATGCCGTCT 3'	55℃, 35 cycles, 785 bp
Ptx3	F: 5' GGAATCGCTACCCTGACATGAG 3' R: 5' TGAAGGCGAACGGGAAGGTCT 3'	60℃, 35 cycles, 276 bp
GFAP	F: 5' TCATCGCTCAGGAGGTCCTT 3' R: 5' CTGTTGCCAGAGATGGAGGTT 3'	58℃, 35 cycles, 353 bp
TuJ1	F: 5' CAACAGCACGGCCATCCAGG 3' R: 5' CTTGGGGCCCTGGGCCTCCGA 3'	58℃, 35 cycles, 244 bp
Otx2	F: 5' CCATGACCTATACTCAGGCTTCAGG 3' R: 5' GAAGCTCCATATCCCTGGGTGGAAAG 3'	50℃, 30 cycles, 211 bp
Girk2	F: 5' GCTACCGGGTCATCACAGAT 3' R: 5' ACTGCATGGGTGGAAAAGAC 3'	60℃, 35 cycles, 162 bp
VMAT2	F: 5' CTTTGGAGTTGGTTTTGC 3' R: 5' GCAGTTGTGATCCATGAG 3'	55℃, 35 cycles, 301 bp
AADC	F: 5' CTCGGACCAAAGTGATCCAT 3' R: 5' GTCTCTCTCCAGGGCTTCCT 3'	58℃, 35 cycles, 212 bp

blocker, to determine nonspecific uptake. After incubation for 10 min at 37°C, the uptake reactions were terminated by aspiration of the reaction solution and washing twice with ice-cold PBS. Cells were lysed with 0.5 M NaOH, and the radioactivity was measured by liquid scintillation counting (MicroBeta® TriLux ver. 4.4 Wallac, Turku, Finland). Specific DA uptake was calculated by subtracting nonspecific uptake (with nomifensine) from the uptake value without nomifensine.

9. Detection of dopamine release by HPLC

High performance liquid chromatography (HPLC) analysis for DA levels was performed as previously described[24] with some modifications. To determine *in vitro* DA release from cultured cells, differentiated precursor cells in 24-well plates were incubated in 500 μl ITS + AA medium with 56 mM KCl for 15 min (evoked release). The media was then collected and stabilized in 0.1 N perchloric acid containing 0.1 mM EDTA, followed by extraction by aluminum adsorption. DA was separated with a reverse phase μ-Bondapak C18 column (150×3.0 mm, Eicom, Japan) at a flow rate of 0.5 ml/min. Electroactive compounds were analyzed at +750 mV using an analytical cell and an amperometric detector (Eicom, Model ECD-300, Japan). DA levels were calculated using an internal standard (50 nM methyl-DOPA) and catecholamine standard mixtures, including 1-50 nM DA (external standard) injected immediately before and after each experiment.

10. Cell counting

Uniform random sampling procedure were used for cell counts and quantified using the fractionator technique.[25] Immunoreactive cells on coverslip cultures were counted on randomly selected microscopic fields in a region of uniform cell growth using an eyepiece grid at a final magnification of 200x or 400x. On each coverslip, 10-20 microscopic fields were counted, and two to four coverslips were analyzed in each experiment.

11. Statistical analysis

Data are expressed as mean ± SEM of at least 3 independent experiments. Statistical comparisons were made by ANOVA, with Scheffe or Tukey post-hoc analysis (SPSS 15.0; SPSS Inc., Chicago, IL) when two or more groups were involved. The paired t-test was applied for comparison of TH+ cells detected using the immunostaining method with or without SDS treatment in identical sections of hES-derived grafts.

III. RESULTS

1. hES-NP is a stable, continuous, and on-demand source for human DA neurons

A. Gradual and synchronous neural differentiation of hES cells by co-culturing with MS5 stromal feeder

Dopaminergic differentiation of hES cells is induced by co-culture on a feeder layer of PA6 or MS5 stromal cells (Fig. 1a).[10,12-14] Human ES cell colonies on the stromal cells differentiated into colonies with primitive neuroepithelial cell structures (Fig. 1b-c).[13,14] We repeatedly subcultured the differentiating hES colonies by splitting them into small colonies (50-500 cells/colony) and replating onto freshly prepared MS5 cells during the co-culture step. The percentage of differentiated colonies with primitive neural structures (NP colonies) gradually increased at each cell passages. Specifically, 15%, 39%, and 87% of hES colonies included NP colonies after the 3rd, 4th, and 5th passages on MS5 cell feeder, respectively (1,000-3,000 colonies from 2-3 independent experiments were examined for each value). Although similar hES differentiation was achieved on a feeder of PA6 cells, a subpopulation of differentiated hES colonies on PA6 (but not on MS5 cells) contained cells with fully mature neuronal morphology (Fig. 1d-e).[10,12] This finding indicates that more synchronous hES cell differentiation, with homogenous populations of cells at the same developmental stage, is likely achieved with MS5 cells than with PA6 cells. All of the following results, therefore, were obtained with hES differentiation on MS5 feeder cells.

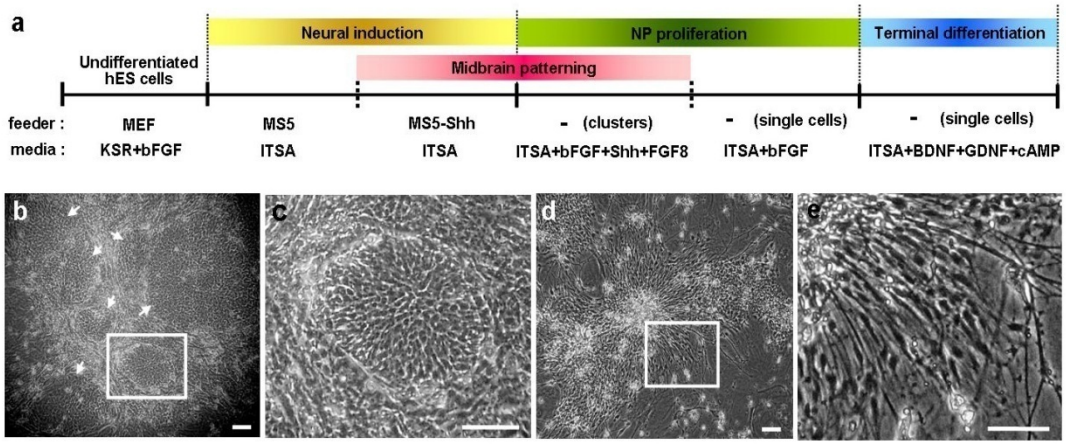

Figure 1. Stromal feeder-induced derivation of neural precursor cells and DA neurons from hES cells. (a) Schematic procedures of DA neuron differentiation. Differentiated hES colonies with neural structures on the stromal feeder MS5 (b, c) and PA6 (d, e). Images (c) and (e) are high-magnification views of the boxed regions in (b) and (d), respectively. Cultures of hES cells on MS5 stromal feeders are uniformly comprise of colonies with primitive neuroepithelial structure (NP colony) that are compactly arranged with small cells with abundant cytoplasm and a barely visible nucleus (b, c). Arrows indicate NP colonies. By contrast, a subpopulation of colonies on PA6 cells is assembled by fully differentiated neuronal cells with multiple extensive processes (d, e). Scale bar, 40 μm.

B. Multi-passaged undifferentiated hES cells lose their differentiation potential

We previously demonstrated that the efficiency of hES differentiation into neural lineages is affected by hES cell lines.[13] In addition, we observed that hES differentiation was also dependent on various experimental conditions, including the size of hES cell colonies, cell viability, and general conditions of the feeder cells (data not shown). In particular, the degree of hES differentiation greatly varied depending on the passage number of undifferentiated hES cells, even in the same HSF-6 hES cell line. In hES cells with an extended passage number [maintained longer on the mouse embryonic fibroblasts (MEF) maintenance feeder], it took longer to achieve hES differentiation (in which >80% of hES colonies differentiated into NP colonies), and such a level of differentiation could not be obtained with hES cells maintained over 75 passages (ES P75; Fig. 2a). Chromosomal analysis of the multi-passaged HSF-6 hES cells with lack of *in vitro* neural differentiation demonstrated multiple chromosomal aberrations (Fig. 2b), indicating that the decreased differentiation capacity of late-passage hES cells is probably associated with chromosomal alterations. These findings collectively suggest that long-term expansion of hES cells with multiple ES passages is problematic to be applied in large-scale generation of hES-derived neural lineage cells.

C. Sustained neural precursor cell properties of hES-NP after expansion *in vitro*

When cultures contained >85% NP colonies, they were transferred as small clusters into FN-coated plates in ITS + AA supplemented with bFGF and were cultured for 7-9 days..The NP clusters were then dissociated into single cells, plated, and cultured in ITS+AA+bFGF (NP passage 1). After 7 days of bFGF-proliferation, over 90% of the total cells were positive for nestin, an intermediate filament specific to neural precursors[13]

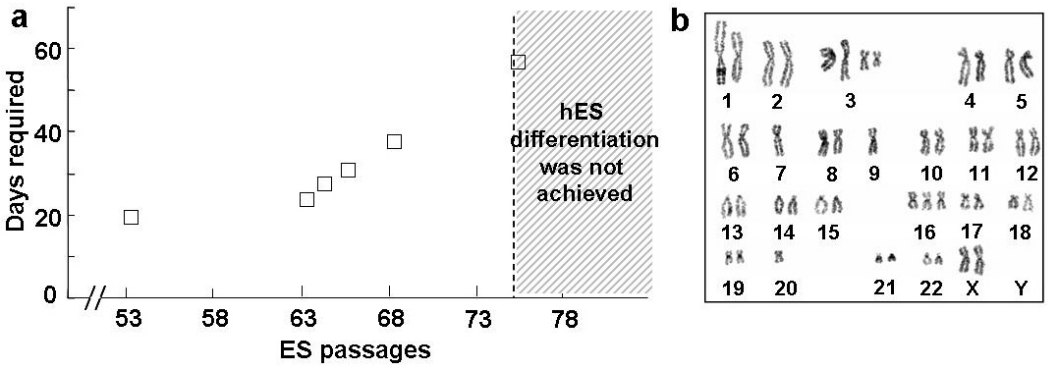

Figure 2. Loss of differentiation potential and chromosomal anomaly of hES cells after long-term culture. (a) Neural differentiation potential of hES cells is lost after long-term culture for maintenance and propagation of undifferentiated hES cells (HSF-6). The graph depicts the number of days required for hES differentiation (>80% of hES colonies are differentiated neuroepithelial cell colonies). (b) Karyotype of the undifferentiated HSF-6 hES cells with ES passage 82. Variable structural and numerical chromosome abnormalities are shown.

(data not shown). Only an extreme minority of cells were negative for HN, suggesting the effective elimination of the feeder cells through mechanical passage followed by selective survival and proliferation of neural precursors. These finding suggest the derivation of an enriched population of neural precursor cells from hES cells. Uniform population of neural precursor cells was similarly derived from the hES cell line H9 by co-culturing with MS5.[14]

hES-NP cells were continuously expanded in the presence of bFGF for 42 days (a total of 6 passages), with the total population doubling level being 14.3 (2.0×10^4-fold increase in total cell number; doubling time, 2.94 days; Fig. 3a). The cell expandability at each passage did not vary significantly during the NP propagation period: for instance, the population doubling level of passage 6 (P6) NP cell culture was similar to that of the P1 NP culture (2.22 in P6 versus 1.74 in P1, Fig. 3b). Normal karyotype was maintained in hES-NP cells during the NP cell expansion (Fig. 3c).

Immunocytochemical analyses revealed that, 92.5±1.8% and 84.6±3.1% out of total cells were positive for nestin and Ki67, a proliferating cell marker, at the NP passage 2, respectively (Fig. 4a, g). Most of the nestin+ cells co-expressed the proliferating cell marker Ki67 (nestin+/Ki67+ out of total nestin+ cells: 93.2%), and nestin+ cell populations were maintained at 90.2-93.1 % during the 6-NP passage period. Comparable results were obtained with the passaged NP cells derived from H9 hES cells (Fig. 5a-d). LeX, known as SSEA-1 or CD15, is an extracellular matrix carbohydrate expressed by mouse ES cells.[26] Recent studies have demonstrated a specific expression of LeX in adult and embryonic rodent neural stem or precursor cells.[27-28] LeX expression was detected in 47.6±3.3% of cells at this NP stage of hES cell differentiation (Fig. 4d, g). Such the lower population of LeX+ cells, compared to nestin+ cell population, might be attributable to a

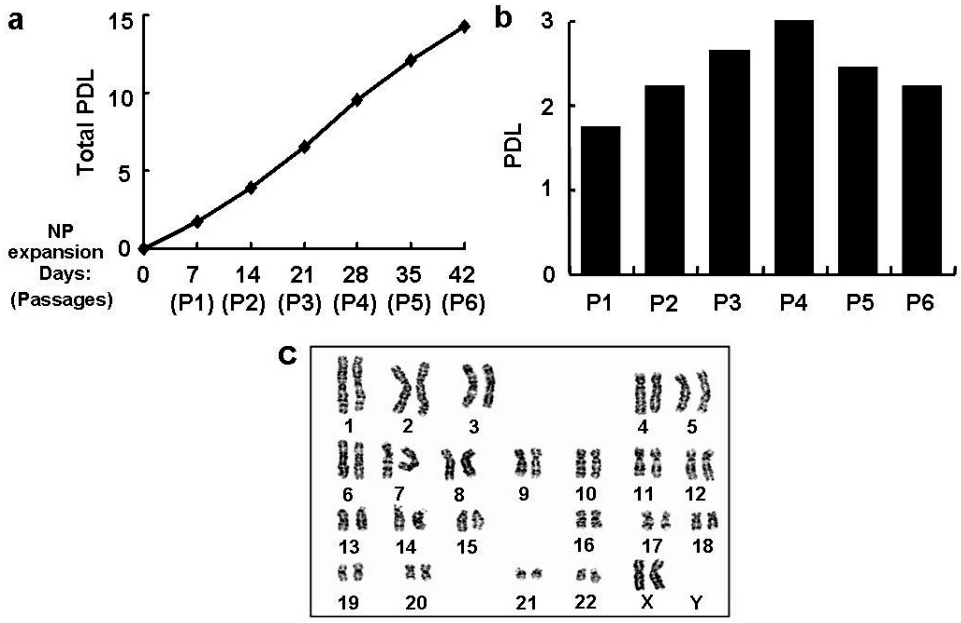

Figure 3. *In vitro* expansion of hES-derived NP cells. (a) Cumulative total population doubling level (PDL). (b) PDL of each NP culture at different NP passage numbers. NP cells derived from hES cells (hES-NP) were cultured with bFGF and passaged every 7 days for 42 days (total of 6 passages). The PDL was calculated as described in 'Materials and Methods'. (c) Normal karyotype of hES-derived NP cells was maintained after 5 times of NP passages.

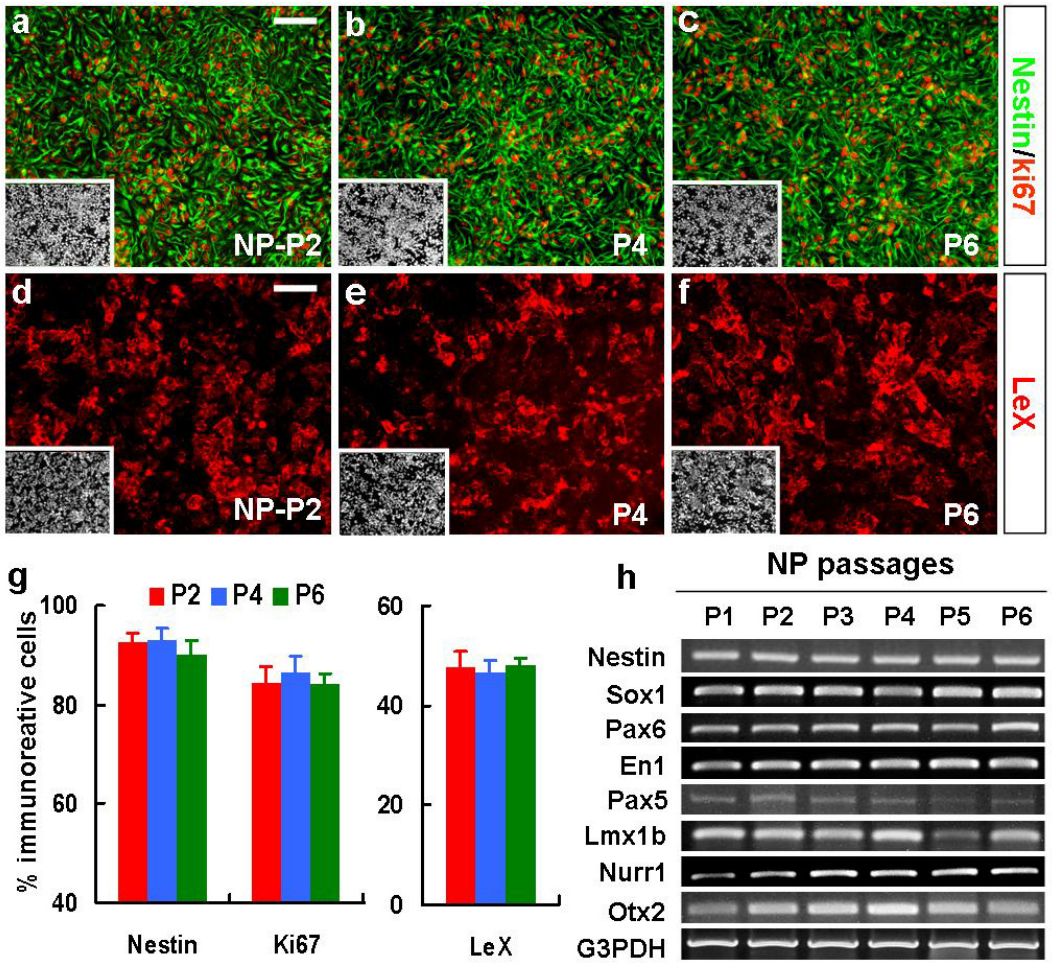
a
b
c
NP-P2
P4
P6
Nestin/ki67
d
e
f
NP-P2
P4
P6
LeX
g
P2 P4 P6
% immunoreative cells
100
80
60
40
60
40
20
0
Nestin
Ki67
LeX
h
NP passages
P1 P2 P3 P4 P5 P6
Nestin
Sox1
Pax6
En1
Pax5
Lmx1b
Nurr1
Otx2
G3PDH

Figure 4. Maintenance of neural precursor cell properties of HSF-6 hES-NP cells during NP cell expansion. HSF-6 hES-NP cells at different NP passage numbers were proliferated *in vitro* in the presence of bFGF, and samples for immunocytochemical (a-g) and RT-PCR (h) analyses were prepared on the last day (day 7) of bFGF-proliferation. (a-f) Immunocytochemical analyses for nestin/Ki67 (a-c) and LeX (surface marker for neural precursor cells, d-f). Each panel in (a-f) is a representative image for nestin+, Ki67+ and LeX+ cells in the cultures for hES-NP cell with NP passage P2, P4, and P6. Insets, DAPI staining of the same field. Graph (g) depicts the percent of cells immunoreactive for nestin, Ki67 and LeX of the total (DAPI+) cells. Note that the proportion of proliferating neural precursor cells in the hES-NP cultures did not significantly alter after NP cell passages. Scale bar, 40 μm. (h) Semi-quantitative RT-PCR analyses for genes specific to neural precursors (nestin, Sox1, and Pax6), midbrain development (En1, Pax5), midbrain dopaminergic markers (Nurr1 and Lmx1b) and forebrain and midbrain development (Otx2). The expression patterns shown are representatives of 3-6 experiments with two RNA samples independently prepared.

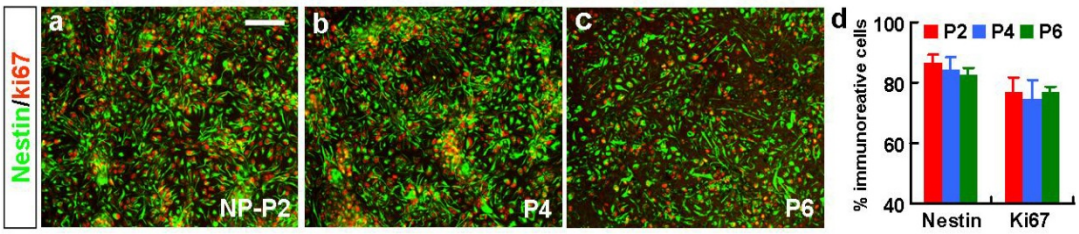

Figure 5. Unaltered phenotypic of H9 hES-derived NP cells after multiple NP passages. H9 hES-NP cells at different NP passage numbers were proliferated *in vitro* in the presence of bFGF as described in 'Materials and Methods', and immunocytochemical analyses for nestin/Ki67 were performed on the last day (day 7) of bFGF-proliferation. Shown are images for cells positive for nestin/ki67 (a-c) after NP expansion. Graph (d) depict the percent of cells positive for nestin/ki67.

matter of sensitivity of LeX antibody used in this study, in the immunocytochemical detection of the expressing cells. However, it may also suggest that LeX expression in human NP cells is restricted to a certain NP cell subpopoulation, while nestin is expressed in a wide range of NP cells including early NP, definite NP and committed progenitor cells. The percentages of LeX-expressing cells were also not significantly altered during the 6 times of NP passages (P2: 47.6±3.3% and P6: 47.9±1.6%, Fig. 4d-g).

We did not observe significant nestin, Sox1, and Pax6 mRNAs level differences by semi-quantitative RT-PCR among hES-NPs with different NP passage numbers (Fig. 4h). Similarly, no obvious NP-passage number-dependent changes in Nurr1, Lmx1b (markers for midbrain DA neuron), and En1, Pax5 (midbrain development), Otx2 (forebrain and midbrain development) could be detected.

D. Sustained neuron/astrocyte yields from late hES-NP cells

To examine whether the differentiation potential of hES-NP cells is altered during *in vitro* expansion, terminal differentiation of hES-NP cells at each NP passage was induced for 6-8 days. NP cells derived from HSF-6 and H9 hES cells at NP passage 2 exhibited high neuronal differentiation with neuronal marker TuJ1-expressing cells being 59.7±2.8% (HSF-6) and 55.4±0.5% (H9) of total cells in the differentiated cultures, whereas only 8.6±1.5% (HSF-6) and 8.8±3.1% (H9) of cells expressed the astrocyte- specific protein GFAP (Fig. 6a, g and Fig. 7a, d). None of cells was positive for CNPase or O4, oligodendrocytic markers tested. These findings suggest an early developmental property of the hES-derived NP cells, given that neural precursors sequentially yield neuron, astrocytes and oligodendrocytes in the developing brain.[29-31] TuJ1+ neuronal and GFAP+ astrocytic yields were not significantly altered after multiple NP passages (Fig. 6a-c, g

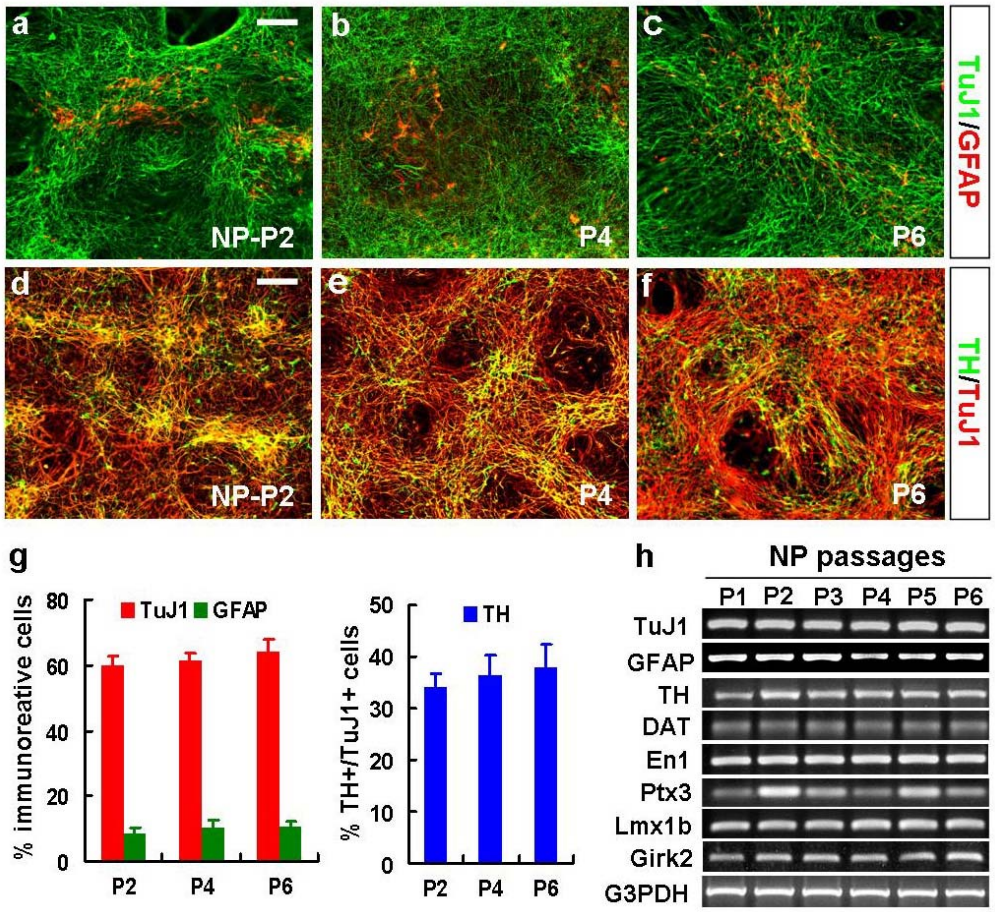

Figure 6. Differentiation phenotypes of HSF-6 hES-NP cells with different NP passages. After 6-8 days of *in vitro* differentiation, phenotypes of the differentiated cultures were assessed by immunocytochemical (a-g) and RT-PCR (h) analyses. (a-f) Representative images for cells positive for TuJ1 (neuronal)/GFAP (astrocytic marker, a-c) and TuJ1/TH (DA neuronal, d-f) of differentiated HSF-6 hES-NP cells at P2, P4, and P6. Scale bar, 40 μm. Graph (g) depicts the percent of cells immunoreactive for TuJ1 and GFAP of the total (DAPI+) cells or TH of the total TuJ1+ cells. (h) Semi-quantitative RT-PCR analyses for the genes specific to DA neuron (TH, DAT), midbrain DA (En1, Ptx3, Lmx1b), A9 midbrain DA (Girk2), neuron (TuJ1) and astrocyte (GFAP).

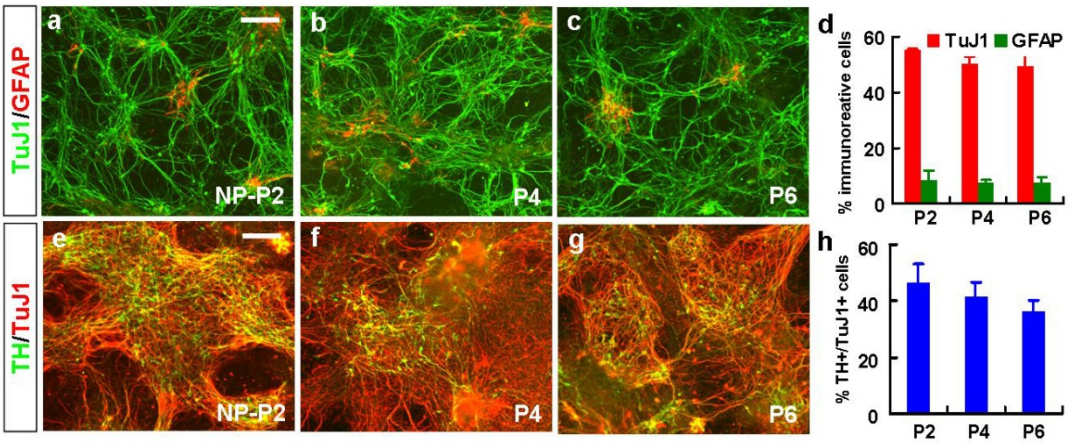

Figure 7. Differentiation properties of H9 hES-derived NP cells after multiple NP passages. To determine the differentiation phenotypes of the NP cells, terminal differentiation of H9 hES-NP cells at each NP passage was induced for 6-8 days. Shown are representative images for cells positive for TuJ1/GFAP (a-c), TH/TuJ1 (e-g) after NP differentiation. Scale bar, 40 μm. Graph (d) and (h) depict the percent of cells positive for TuJ1/GFAP, and TH/TuJ1, respectively.

and Fig. 7a-d): for instance, percents of TuJ1+ cells out of total (DAPI+) cells: 59.7±2.8% (NP-P2), 61.2±2.6% (P4), 64.3±3.7% (P6); GFAP+ cells: 8.6±1.5% (P2), 10.4±2.0% (P4), and 10.8±3.7% (P6) in the differentiated HSF-6 hES-NP cultures. This result is in a contrast to the differentiation of NP cells isolated from rodent embryonic brain demonstrating rapid neuron-to-astrocyte switch during their *in vitro* cell expansion.[32]

E. DA neuron subtype differentiation

This study focused on hES-NP differentiation towards DA neurons, a neuronal subtype clinically relevant to psychiatric or neuro-degenerative disorders such as PD. Consistent to previous studies,[13-14] large population (HSF-6: 34.0±2.9%, H9: 44.5±6.6% at P2) of TuJ1+ neurons co-expressed TH, a DA neuronal marker. Dopamine β-hydroxylase (DBH), a noradrenergic or adrenergic neuronal marker, did not colocalize with TH+ cells (data not shown), suggesting a DA neuronal identity of the hES-derived TH+ cells. It has been demonstrated that NP-derived DA neuron yield was nearly completely lost after one to two times cell passages in the cultures derived from rodent embryonic ventral midbrain.[33-34] In a clear contrast, hES-NP cells efficiently yielded TH+ neurons after 4-6 times of NP cell passages. A large difference was not observed in TH+ cell yield depending on NP cell passage. Instead, the percent of TH+ cells out of the TuJ1+ neurons was slightly greater in late NP cells (36.6±3.6% at P4 and 38.0±4.5% at P6, compared to 34.0±2.9% at P2). Semi-quantitative RT-PCR analyses for TuJ1, GFAP, and TH further supported unaltered neuron/astrocyte and DA neuronal differentiation over the hES-NP cell passages (Fig. 6h). Furthermore, mRNA expressions of the genes specific for other DA neuronal (DA transporter, DAT), midbrain dopaminergic (En1, Ptx3, Lmx1b), A9

midbrain-specific dopaminergic (Girk2) markers were not greatly varied in the cultures at different NP cell passages (Fig. 6h). Maintenance of high DA neuron yields after prolonged NP cell expansion has been similarly shown in the differentiation of H9 hES-NP cells (Fig. 7e-h).

In addition to coexpression of TH/TuJ1 (Fig. 6d-f), human-specific neuronal (HuC/D and hNCAM, Fig. 8b, c) and mature neuronal (MAP2, Fig. 8d) markers were expressed in virtually all TH+ cells derived from multi-passaged hES-NP cell cultures (P6, HSF-6 hES-NP). Synapse formation and neurotransmitter homeostasis are definite properties acquired in mature functional pre-synaptic neurons. Synapsin, a synaptic vesicle-specific protein, was co-localized in TH+ fibers in the differentiated hES-NP cultures (Fig. 8e). In addition to DAT mRNA expression shown in Fig. 6h, TH+ cells in the multi-passaged hES-NP cultures expressed another DA neurotransmitter homeostasis protein VMAT2 (Fig. 8f). These findings indicate well-differentiated mature DA neuronal properties of hES-derived TH+ cells.

Fig. 4h and 6h demonstrated unaltered expressions of the mRNAs specific to midbrain developmental and midbrain DA neuronal genes over NP cell passages in hES-NP-derived cultures. Consistently, cells immunoreactive for the midbrain DA neuron-specific markers En1 and Nurr1 and midbrain-specific marker Pax2, and Pax5 were readily detected in the differentiated cultures for the multi-passaged hES-NP cells (P6, HSF-6 hES-NP). Consistent to the previous studies,[14] Nurr1 and En1 were localized in a subpopulation of TH+ cells (Fig. 8g and h) whereas Pax2- and Pax5-expressing cells were negative for TH (Fig. 8i and j). Calbindin is a calcium-binding protein, of which expression in midbrain DA neurons is related to increased resistance to cell death in PD.[35-37] Another line of studies has demonstrated a specific expression of calbindin in DA

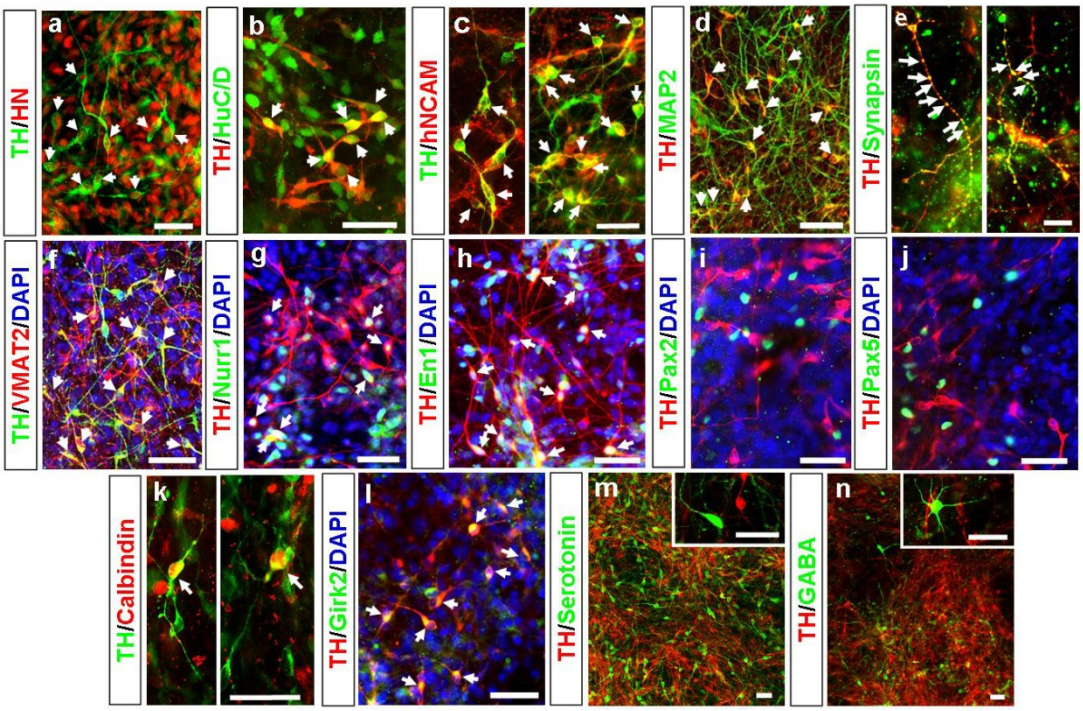
TH/HN
a
TH/HuC/D
b
TH/hNCAM
c
TH/MAP2
d
TH/Synapsin
e
TH/VMAT2/DAPI
f
TH/Nurr1/DAPI
g
TH/En1/DAPI
h
TH/Pax2/DAPI
i
TH/Pax5/DAPI
j
TH/Calbindin
k
TH/Girk2/DAPI
l
TH/Serotonin
m
TH/GABA
n

Figure 8. Immunocytochemical phenotypes of multi-passaged hES-DA cells. HSF-6 hES-NP cells at NP passage 6 were differentiated for 6-8 days, and subjected to double immunocytochemical analyses for TH/HN (a), TH/HuC/D (b), TH/hNCAM (c), TH/MAP2 (d), TH/Synapsin (e), TH/VMAT2 (f), TH/Nurr1 (g), TH/EN1 (h), TH/Pax2 (i), TH/Pax5 (j), TH/Calbindin (k), TH/Girk2 (l), TH/Serotonin (m), and TH/GABA (n). Right and left images in (c) and (k) were taken from two isolated microscopic fields. Scale bar, 20 μm. Co-labeled cells were indicated as arrows. Note that all or most of TH+ cells express HN, HuC/D, hNCAM, (human-specific neuronal), MAP2 (mature neuronal), and VMAT2 (DA homeostasis). By contrast, midbrain-specific markers Pax2 and Pax5 expressions are separated from TH (i and j), whereas midbrain DA-specific markers Nurr1, En1 and Girk2 co-localized in subsets of TH+ cells (g, h and l). Insets of (m) and (n), the high-powered images. Note that cells immunoreactive for TH and GABA are well separated, of which co-localization is a characteristic feature of olfactory (forebrain) or developing striatal DA neurons.

neurons of the ventral tegmental area (A10), but Girk2 in DA neurons of the substantia nigra (A9).[38-40] Consistent with previous studies,[13,41] only a minor proportion (<1%) of TH+ cells expressed calbindin (Fig. 8k). Girk2 mRNA expression in differentiated hES-NP cell cultures was evident (Fig. 6h) and Girk2 was co-labeled TH+ neurons differentiated from hES-NP (Fig. 8l). DA and serotonin neurons in mouse brain development are simultaneously generated in the ventral parts of the midbrain and hindbrain, respectively, by common combinational actions of SHH and fibroblast growth factor 8 (FGF8).[42] The co-generation of these two neurotransmitter neuronal subtypes was also shown in mouse ES differentiation *in vitro*.[43] Consistently, serotonin+ neurons were another major neuronal population in the differentiated hES-NP cultures (21-25 % of TuJ1 neurons), and the percentage of serotonin neurons was not significantly altered after multiple NP cell passages (Fig. 8m and data not shown). In accordance with previous studies for hES cell differentiation, the GABA+ neuronal population was relatively minor (8-10 %, Fig. 8n). No cell passage-dependent variation in GABA+ neuron numbers was observed (data not shown). GABA and TH co-expression is a characteristic feature of olfactory DA neurons[44] and transiently observed in striatal GABAergic neurons.[45] No co-expression of GABA and TH was observed, further supporting midbrain dopaminergic differentiation of hES-NP cells.

In vitro functions as pre-synaptic DA neurons were examined by the assays for DA neurotransmitter release and uptake. HPLC analyses revealed that differentiated P2, P4 and P6 hES-NP cells released considerable amounts of DA upon KCl-induced depolarization: 7.25±0.46 (P2); 6.86±0.73 (P4); 5.93±0.80 (P6) pg/15 minutes/TH+ cell (Fig. 9a, b). DAT-mediated high affinity reuptakes of DA were 0.23±0.05 at P2, 0.26±0.01 at P4, and 0.27±0.06 fmol/minute/TH+ cell at P6 (Fig. 9c). The DA release and

uptake values were not significantly different in the cultures at different passages (p values shown in Fig. 9b, c). These findings collectively indicate maintenance of developmental potential of hES-NP cells towards mature functional midbrain-type DA neurons after multiple NP cell passages.

F. Storage of hES-NP cells in liquid nitrogen

hES-NP cells at every passage were stored in bFGF-supplemented medium containing 10% dimethyl sulphoxide (DMSO) in liquid nitrogen (LN_2) and re-cultured by a simple freezing/thawing method. When LN_2-stored cells from NP passage 5 and 6 were thawed for re-culture, 78.6±2.5% and 77.5±3.3% of cells were viable 5 hours after plating, respectively (n=16 for each value). The result was in clear contrast to the poor viability of undifferentiated hES cells when re-cultured from LN_2-storage (data not shown). The proliferative and DA neurogenic potentials of hES-NP cells were not significantly altered after several freeze-thaw cycles (Fig. 10 and data not shown). Furthermore, long-term storage (at least up to 20 months) did not abrogate NP cell properties (data not shown). These findings provide another substantial benefit of hES-NP cells serving as a continuous, on-demand source of human NP cells or DA neurons.

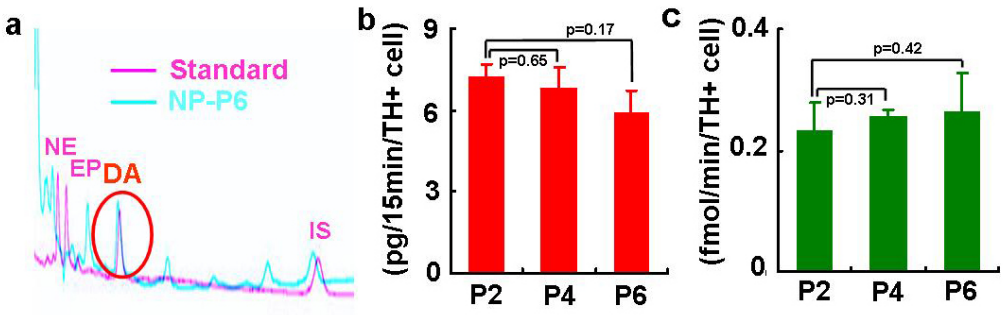

Figure 9. *In vitro* presynaptic neuronal functions of DA cells differentiated from hES-NP cells at NP passage 2, 4 and 6. (a) Typical HPLC chromatogram for DA released from differentiated NP-P6 (blue) is shown with that for mixture of standards (NE, norepinephrine; EP, epinephrine; DA, red). IS represents internal standard (3,4-dihydroxybenzylamine) used for quantification of DA concentrations. The graph (b) shows DA levels in the medium supplemented with 56 mM KCl. (c) DAT-mediated specific DA uptake. DA uptake was calculated by subtracting non-specific uptake (with nomifensine) from the total uptake (without nomifensine). The level of DA release and uptake per TH+ cell was calculated by dividing each value by the TH+ cell number obtained from cultures conducted in parallel to the DA release and uptake assays. The boxes and bars in graph (b) and (c) represent means and standard errors of DA releases (n=8) and DA uptakes (n=6). p values indicated were obtained in one-way ANOVA by comparing with the DA release and uptake values of P2 cultures.

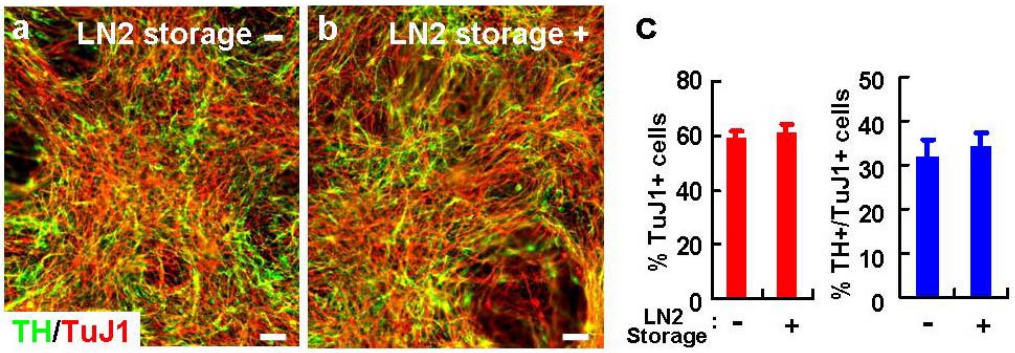

Figure 10. **Unaltered DA neuronal yield of hES-NP cells after freeze-and-thaw cycle.** After 4 NP cell passages, the hES-NP cells continued to be cultured or frozen in LN_2. One week after the LN_2 storage, cells were thawed and re-cultured. TuJ1+ neuronal and TH+/TuJ1+ DA neuronal yields of the LN_2-stored cells at P6 were compared with those directly cultured without frozen in LN_2 at the same passage number. No significant differences in TuJ1+ and TH+/TuJ1+ cell numbers was observed between the cultures with (+) and without (-) LN2 storage (a-c).

2. Cell survival and tumor formation after hES-NP cell transplantation

A. Proportions of potentially tumorigenic cells in hES-NP cell cultures

Our protocol for derivation of hES-NP cells includes (a) neural induction on the MS5 stromal cell feeder, (b) ventral midbrain patterning by treatment with SHH + FGF8,[42] (c) successive subculturing of completely dissociated cell preparations, and (d) expansion of NP cells with bFGF. The yield is a highly homogeneous (>95% nestin-positive cells) population of midbrain-type NP cells which terminally differentiate into DA neurons co-expressing the midbrain DA neuron markers, En1, Nurr1 and Girk2 (Fig. 8l). The population remains homogenous and DA neuron-enriched through multiple cycles of passage and expansion as required of a stable and renewable cell source for transplantation. For successful therapy, however, donor cells must be free of tumorigenicity and able to survive *in vivo*. To test the first requirement, we determined the proportions of undifferentiated hES cells and the cellular composition of neural rosettes (neuroepithelial cells), both reported to generate tumors (e.g., teratomas), in hES cell-derived transplants.[10,41,46,47] The hES-NP single cell dissociates, when plated for subculture, reformed numerous rosette structures expressing the NP cell marker nestin and the proliferating cell marker Ki67 during the first three passages (Fig. 11a, b). However, numbers of these primitive neuroepithelial structures were decreased during 2-4 passages of NP cell expansion (7.9±0.4/cm^2 at NP-P2 vs 5.4±0.1/ cm^2 at P4, $p < 0.01$ by ANOVA with post-hoc Tukey t-tests; obtained from nine dishes (6cm-) of each passage in three independent experiments), and completely depleted after six passages (Fig. 11c), indicating that the use of late NP cells for transplantation may reduce tumor risk. Appearance of rosette structures in early passages and elimination by several passages

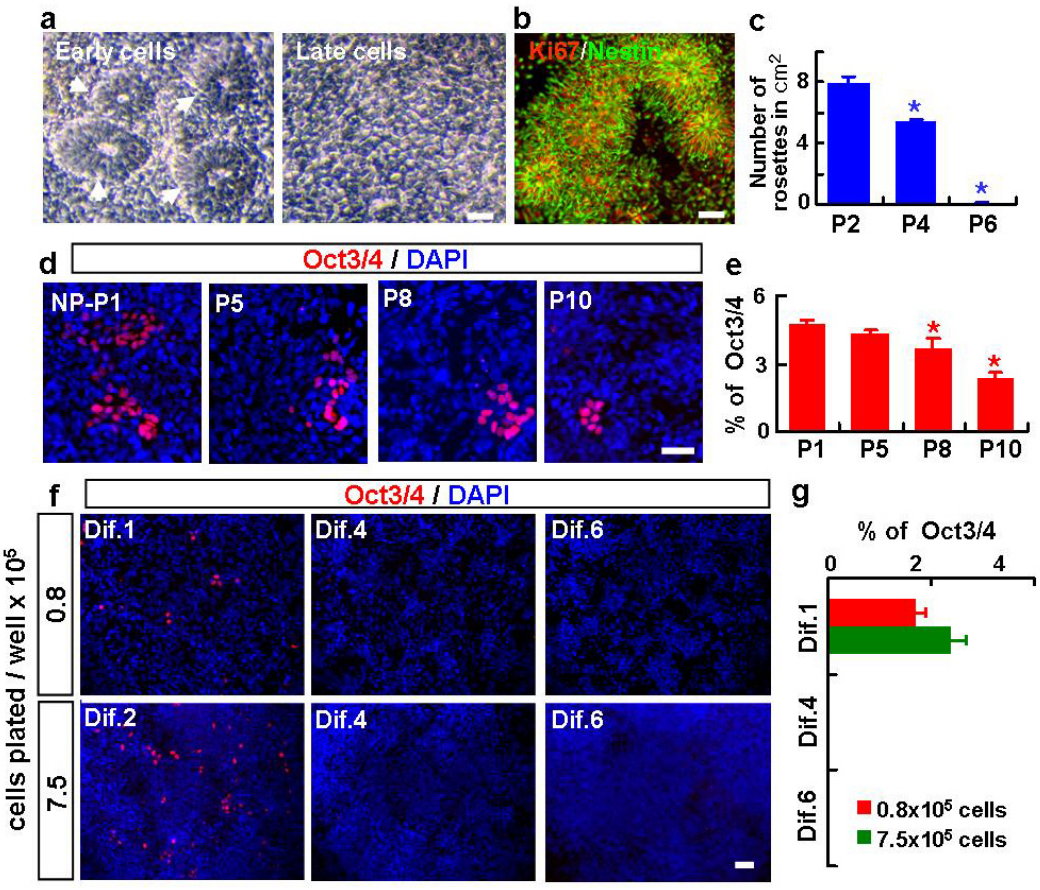
a
Early cells
Late cells
b
Ki67/Nestin
c
Number of rosettes in cm2
8
4
0
*
*
P2
P4
P6
d
Oct3/4 / DAPI
NP-P1
P5
P8
P10
e
% of Oct3/4
6
3
0
*
*
P1
P5
P8
P10
f
Oct3/4 / DAPI
cells plated / well x 10^5
0.8
7.5
Dif.1
Dif.4
Dif.6
Dif.2
Dif.4
Dif.6
g
% of Oct3/4
0
2
4
Dif.1
Dif.4
Dif.6
0.8x10^5 cells
7.5x10^5 cells

Figure 11. Proportion of potentially tumorigenic cells in hES-NP cell cultures. Neural rosette formation (a-c) and proportions of Oct3/4+ undifferentiated hES cells (d-e) in expanded hES-NP cultures at sequential cell passages**.** The hES-NP cells were passaged every 7 days in the presence of bFGF by dissociation into single cells and plating on PLO/FN-coated dishes. Images in (a) are the representative phase-contrast microscopic views of hES-NP cultures at NP-P2 (left) and P6 (right); (b) immunofluorescent view of nestin+/Ki67+ neural rosette structures in hES-NP at P2; (c) graph of numbers of rosettes counted; (d) representative images of Oct3/4+ cells in hES-NP cultures at P1, P5, P8, and P10; (e) the percent of total cells that were Oct3/4+. Significantly different from NP passage 2 (or 1) at $p < 0.01$*. f and g, proportion of Oct3/4+ cells among directly differentiating hES-NP cells. NP-derived cells from P5 were dissociated, plated at 0.8×10^5 and 7.5×10^5 cells/well (a cell density identical to that of donor cell solutions used for transplantation; see Materials & Methods), and directly differentiated in the absence of bFGF for 1, 4 and 6 days. Note that there are no Oct3/4+ cells after culturing under bFGF-free conditions for 4 or 6 days. Scale bar, 40 μm.

were invariable shown regardless of hES cell line (HSF6, H9) and hES-NP cell stock. By contrast, proportions of undifferentiated hES cells detected by Oct3/4-immunostaing were highly variable (0-5% out of total cells) in hES-NP cells generated by different round of hES cell differentiation. Thus, experiments were followed using hES-NP cell stocks containing high percentages of Oct3/4+ cells. A proportion of cells (4.8±0.1%, n=3, 90 microscopic fields from 9 cultured coverslips of 3 independent experiments) expressed the undifferentiated hES cell marker, Oct3/4, when determined 4 days after bFGF expansion of NP-P1 (Fig. 11d, e). These Oct3/4+ cells gradually decreased over passages (for example, 2.4±0.2% at P10, significantly different from P1 at $p < 0.01$), but did not completely disappear even after 10 cycles of complete dissociation and replating in the cell passage procedure.

Although cells were initially plated in the form of single cell dissociates, virtually all Oct3/4+ cells assembled into cell clusters. The presence of such clusters suggests that dissociated Oct3/4+ cells have the potential to survive and proliferate. Given that bFGF is indispensable for the maintenance and proliferation of undifferentiated hES cells, this factor could be considered most important for the survival/proliferation of Oct3/4+ cells. Thus, to more appropriately predict the possibility of teratomas after hES-NP cell transplantation, we re-evaluated the proportion of Oct3/4+ cells after culturing in the absence of bFGF, a condition that mimics the *in vivo* environment of the transplant where high levels of bFGF are unlikely. One day after plating hES-NPs in bFGF-free media, Oct3/4+ cells were detected in the form of dissociated single cells (percent Oct3/4+ cells: 2.1±0.3% at P2, 1.8±0.3% at P5 and 1.4±0.2% at P10, n=3, 90 microscopic fields from 9 coverslips of 3 independent cultures). Surprisingly, after culturing for three more days in the absence of bFGF, Oct3/4+ cells completely disappeared, and did not reappear during

the rest of the culture period (Fig. 11f, g). The disappearance of Oct3/4+ cells followed the same pattern regardless of NP passage number (data not shown), and was also evident in bFGF-free cultures plated at the extremely high cell concentration (7.5×10^5 cells/well in 24-well plates; Fig. 11f lower and g); the number of cells is identical to that used for transplantation (see Materials and Methods).

B. Apoptosis of hES-NP cells after multiple passages in the absence of trophic factors

In most previous studies of hES-DA differentiation,[13,14,48,49] terminal differentiation of hES-NP cells into DA neurons were induced in the presence of differentiation and survival factors such as BDNF, GDNF, and cAMP. In the continued presence of these cytokines, cells survived for more than 15 days of *in vitro* differentiation with no change in viability or apoptotic indices with passage number (data not shown). However, high levels of these trophic factor supports are unlikely in the transplanted brain *in vivo*. Thus an appropriate prediction of hES-NP cell survival and differentiation after transplantation needs to be evaluated in the absence of these trophic factors. Without the supplemental trophic factors, cell viability fell precipitously after more than five passages (late NP), and the cultures failed to survive for longer than 4-6 days of differentiation. Consistently, the indices of apoptosis [estimated by the number of cells with apoptotic nuclei and cells positive for activated (cleaved) caspase-3 (Fig. 12)] gradually increased with passage number. Three days after bFGF withdrawal, for example, the proportions of cleaved caspase 3+ cells in cultures of P1, P5, and P10 were 3.6±0.6%, 7.0±0.4%, and 35.0±0.9%, respectively (for each value, n=3, 90 microscopic fields from 9 coverslips of 3 independent cultures). The proportions of apoptotic nuclei also increased significantly

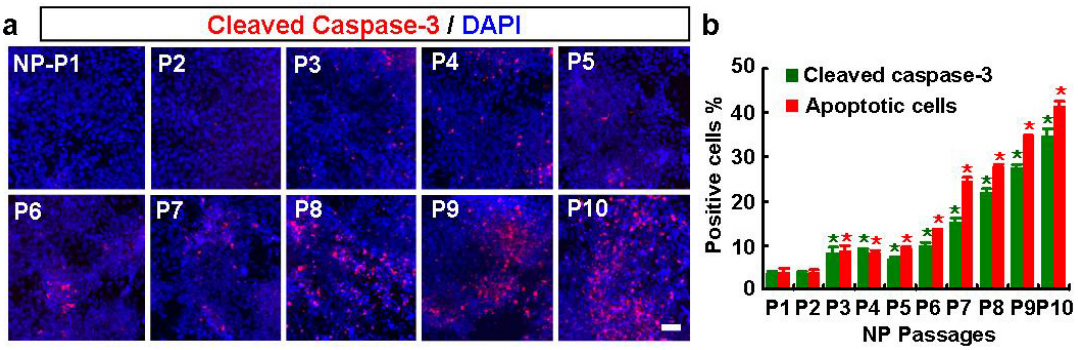

Figure 12. Apoptosis of hES-NP cells upon differentiation increases with passage number. At different passage numbers, hES-NP cells were cultured in the presence of bFGF for 5 days and induced to differentiate by withdrawal of bFGF. At day 3 of differentiation, apoptosis was measured by immunocytochemical analysis for activated (cleaved) caspase-3. Images in (a) are representative for activated caspase-3+ cells in cultures with NP passages 1-10; (b) the percent of cells immunoreactive to activated caspase-3 (green bar) and cells with apoptotic (condensed or fragmented) nuclei (red bar), respectively. * Significantly different from NP passage 1 ($p < 0.01$, n=3, 90 microscopic fields from 9 coverslips, of 3 independent cultures). Scale bar, 40 μm.

(P1: 4.2±0.5%, P5: 9.1±0.4%, and P10: 41.5±1.2%, Fig. 12b). This trophic factor dependence would prohibit the use of the hES-NP cells for transplantation therapy, and this finding guided our subsequent investigation.

C. Effects of BDNF, GDNF, and cAMP on cell survival and DA neuron yields from hES-NP cells

We next examined the contribution of each trophic factor to the survival of differentiating hES-NP cells. Individual treatments of BDNF, GDNF, and cAMP slightly decreased apoptosis (Fig. 13a, b). By contrast, the triple combination of BDNF+GDNF+cAMP dramatically improved cell survival. At differentiation day 3 in P8, the proportions of total (DAPI+) cells that were cleaved caspase-3+ were 11.5±0.7% with the triple treatment and 29.2±1.1% in the control (n=4, 240 microscopic fields from 12 coverslips, of 4 independent cultures; $p < 0.01$); cells with apoptotic nuclei were 11.4±0.6% and 28.0±1.1% of the total in treated and control cultures, respectively ($p < 0.01$).

During 15 days of hES-NP cell differentiation *in vitro,* the numbers of TH+ DA neurons increased gradually. In the absence of the trophic factors, DA neuron differentiation slowed and decreased (Fig. 13c). Surprisingly, but consistent with previous reports,[50-53] TH+ cell numbers in the cultures treated with BDNF or GDNF did not differ significantly from the untreated control. At differentiation day 6, the proportions of TH+ cells were 2.1±0.3% in control cultures, 2.6±0.3% in BDNF ($p=0.92$), and 2.7±0.2% in GDNF ($p=0.83$). By contrast, cAMP treatment greatly enhanced TH+ cell yields (7.3±1.0%; Fig. 13d, e, n=4, 80 microscopic fields from 8 coverslips, of 4 independent cultures; $p < 0.01$). Further improvement of TH+ cell yields was shown with

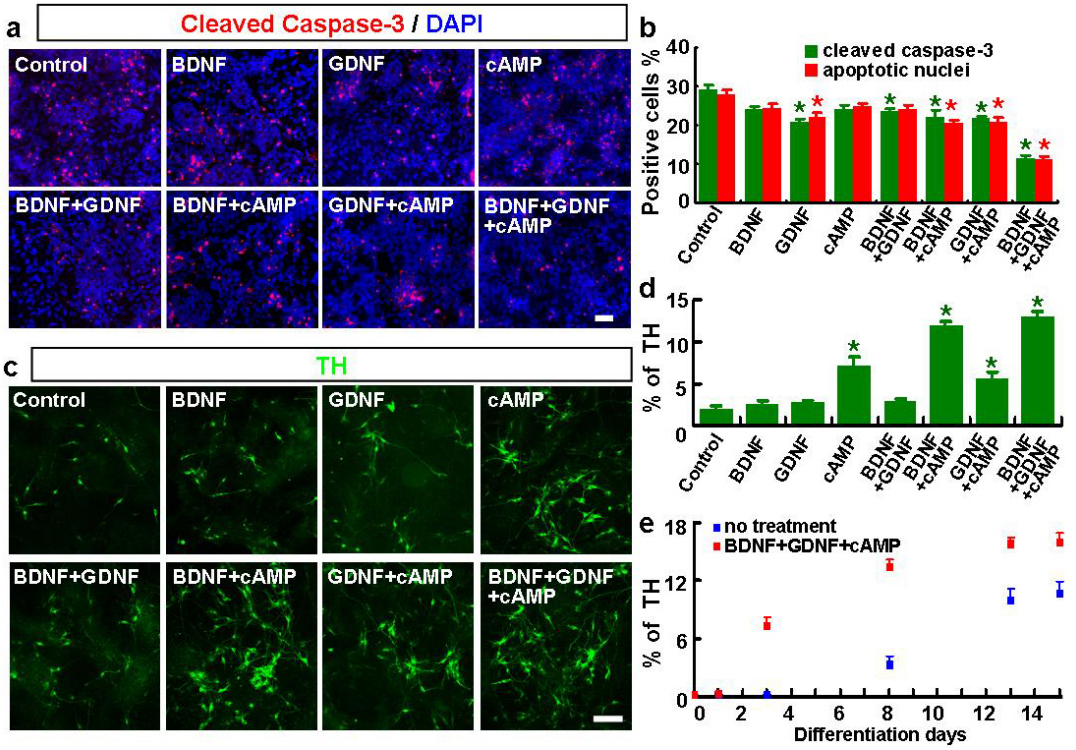

Figure 13. Effects of BDNF, GDNF, and cAMP treatment on survival and differentiation of hES-NP cells with multiple passages. Cell survival (a, b) and DA neuron yields (d, e) were estimated at P8 by the percent of total (DAPI+) cells with cleaved caspase 3+/apoptotic nuclei and positive TH reaction (TH+) 3 days after differentiation in the absence or presence of the cytokines. The percent of early hES-NP cells (P2) that were TH+ was measured (c) over 15 days of *in vitro* differentiation in the presence (red dots) or absence (blue dots) of BDNF+GDNF+cAMP. $p < 0.01$* from the respective control values. Scale bar, 40 μm.

combined treatments of BDNF+cAMP (11.9±0.4%) and BDNF+GDNF+cAMP (13.0±0.6%). In this experimental context, the triple combination of factors provided optimal support for hES-NP cell survival and differentiation *in vitro*.

D. Bcl-XL and SHH improve survival of differentiating hES-derived NP cells

The low viability of cytokine-deprived late hES-NP cells severely limits their potential use as a cell source for transplantation. We therefore explored ways to sustain their survival through manipulation of cell survival-related genes. The Bcl-XL protein, a member of the anti-apoptotic Bcl-2 family, has been shown to prevent cell death in various neuronal populations.[54] In neural precursors[55] and postmitotic neurons, especially midbrain DA neurons,[56] SHH has also been shown to mediate survival. We tested whether transgenic expression of these survival factors could augment the viability of late NP cells. In contrast to the low efficiency of retroviral gene transfer in undifferentiated hES cells (our unpublished data), a retroviral construct efficiently expressed the transduced genes in hES-derived NP cells: 2 days after infection with a retroviral construct expressing GFP, more than 40% of total cells were GFP+ and the expression was sustained for at least 15 days after infection (Fig. 14a, b). Similarly, expression of Bcl-XL and SHH exogenes, estimated by RT-PCR analyses, was robustly induced in hES-NP cells by retroviral gene transfer and stably maintained during the culture period (Fig. 14b). Estimates of cell death and apoptosis by LDH assay (Fig. 14e), staining for PI (Fig. 14c, f) and cleaved caspase-3 (Fig. 14d, g) showed that co-expression of Bcl-XL and SHH enhanced cell survival additively or synergistically in hES-NP cells at P10. Proportions of cells positive for cleaved caspase-3, for example, were 42.2±1.3% (control), 33.0±0.5% (Bcl-XL), 27.0±2.0% (SHH), and 6.5±0.8% (Bcl-XL+SHH).

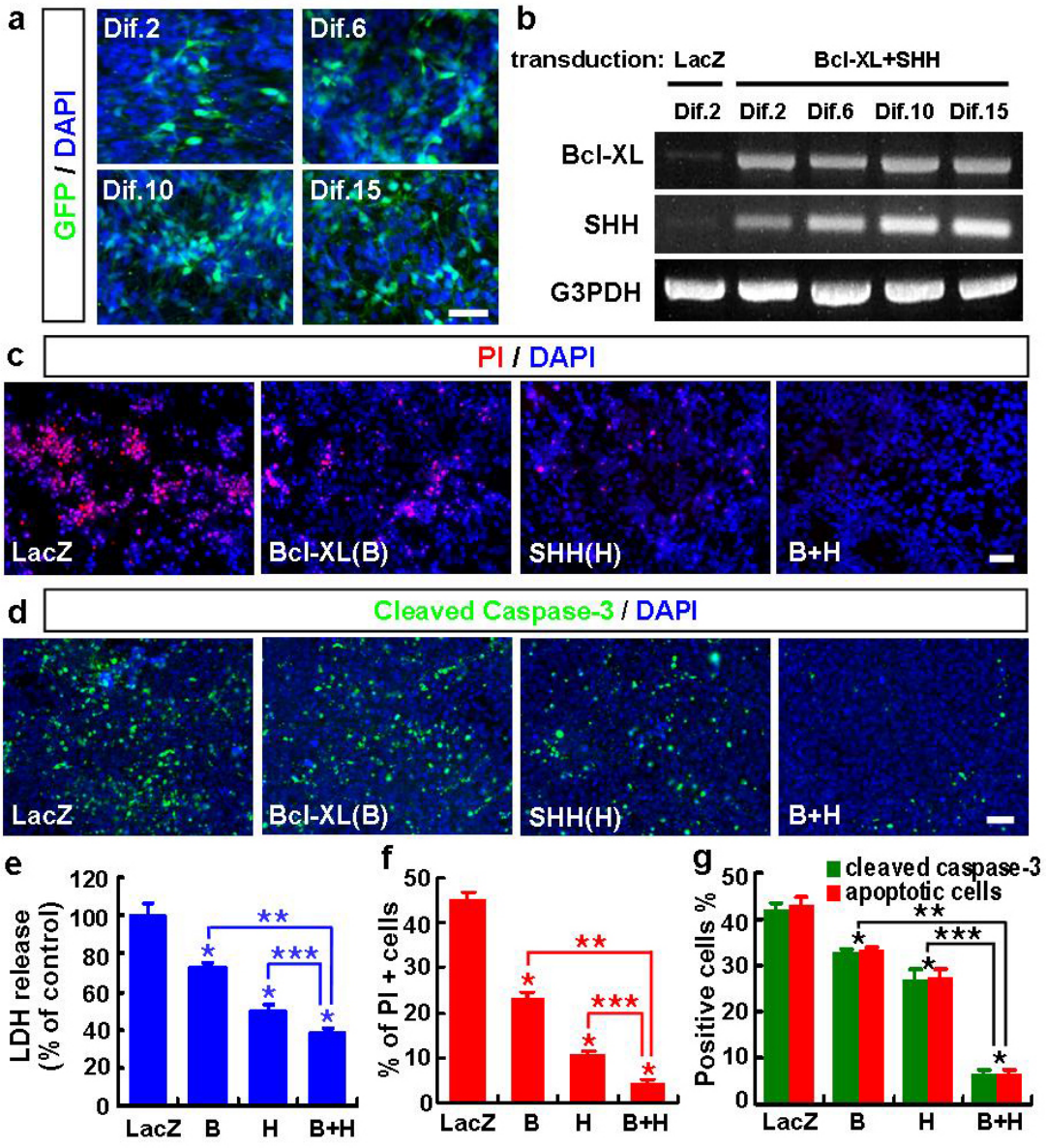
a
GFP / DAPI
Dif.2
Dif.6
Dif.10
Dif.15
b
transduction: LacZ
Bcl-XL+SHH
Dif.2
Dif.2
Dif.6
Dif.10
Dif.15
Bcl-XL
SHH
G3PDH
c
PI / DAPI
LacZ
Bcl-XL(B)
SHH(H)
B+H
d
Cleaved Caspase-3 / DAPI
LacZ
Bcl-XL(B)
SHH(H)
B+H
e
LDH release (% of control)
120
100
80
60
40
20
0
LacZ
B
H
B+H
f
% of PI + cells
50
40
30
20
10
0
LacZ
B
H
B+H
g
cleaved caspase-3
apoptotic cells
Positive cells %
50
40
30
20
10
0
LacZ
B
H
B+H

Figure 14. Transgenic expression of Bcl-XL and SHH in late hES-NP cells prevents cell death and apoptosis. The hES-NP cells at P10 were transduced with retroviruses expressing Bcl-XL and/or SHH as described in 'Materials and Methods.' Differentiation was induced the day following transduction by withdrawal of bFGF, and cell death or apoptosis was analyzed 3 days later. (a) and (b), Efficiency and pattern of exogene expression were estimated in cultures transduced with viruses carrying GFP, Bcl-XL and SHH genes after 15 days of *in vitro* differentiation. Shown in (a) are images of GFP-immunoreactive cells in the cultures at different days after inducing differentiation; (b) RT-PCR analyses of exogenous Bcl-XL and SHH mRNA expression during the course of *in vitro* differentiation. The PCR conditions will be provided upon request. Indices of cell survival/death in cultures transduced with LacZ (control), Bcl-XL (B), SHH (H) or Bcl-XL+SHH. Representative images for PI + cells (c) and activated caspase-3+ cells (d) in the indicated transduced cultures (scale bar, 40 μm); (e) LDH release relative to the respective LacZ-control; (f) percent of cells immunoreactive for PI and activated caspase-3; and (g) percent of cells with apoptotic nuclei. Significantly different from *LacZ-transduced control, ** Bcl-XL-transduced, and *** SHH-transduced at $p < 0.01$. The statistical analyses were made by ANOVA with post-hoc Tukey comparisons (n=12 cultures from 3 independent experiments) for LDH assays, n=3, 60 microscopic fields from 6 cultured coverslips of 3 independent cultures) for PI-stained cells, n=3, 120 microscopic fields from 6 coverslips of 3 independent cultures).

Most importantly, late hES-NP cells (P5-P10) expressing Bcl-XL+SHH (but not Bcl-XL or SHH alone) could survive for more than 15 days of *in vitro* differentiation in the absence of BDNF+GDNF+cAMP. These genetic manipulations, however, did not significantly alter yields of TH+ DA neurons (data not shown).

E. Enhanced survival of Bcl-XL+SHH-transduced hES-NP cells in PD rats

In the final set of experiments, we explored the *in vivo* survival, differentiation, and function of hES-NP cells at early and late passages, and the effects of Bcl-XL+SHH expression in these cells when they were transplanted to the striatum of the rat PD model. The PD rats were randomly assigned into five groups and grafted with naïve early hES-NP cells (NP-P2-P3, n=9, early NP), early NP cells transduced with Bcl-XL+SHH (n=16, B+H early NP), late NP cells (P9-P10, n=7, late NP), and Bcl-XL+SHH-transduced late NP cells (n=16, B+H late NP). An additional group was sham operated (PBS-injected, n=5). The hES-NP cells were injected directly into the rat striatum.

Naïve, nontransduced early NP cells survived in the host striatum and formed masses of grafts along the needle tracts (Fig. 15a, e). Average graft volume in these animals was 1.5±0.5 mm^3 at 8 weeks post-transplantation. The total number of viable donor cells per graft labeled by immunostaining of human nuclear antigen (HN+ cells) was 483,814±128,923 cells (Fig. 15f, j), resulting in a density of 198,167±38,751 HN+ cells per mm^3 in the graft. In contrast, a few HN+ cells were detected occasionally in the striatum of rats grafted with late NP cells (Fig. 15e, h, j). Transplants of late NP cells did not form graft masses at all (Fig. 15c). The survival indices in PD rats grafted with B+H early NP cells did not differ significantly from those of early NP cells (Fig. 15b, e, g, j). By contrast, B+H transduction in late NP cells strikingly enhanced survival indices

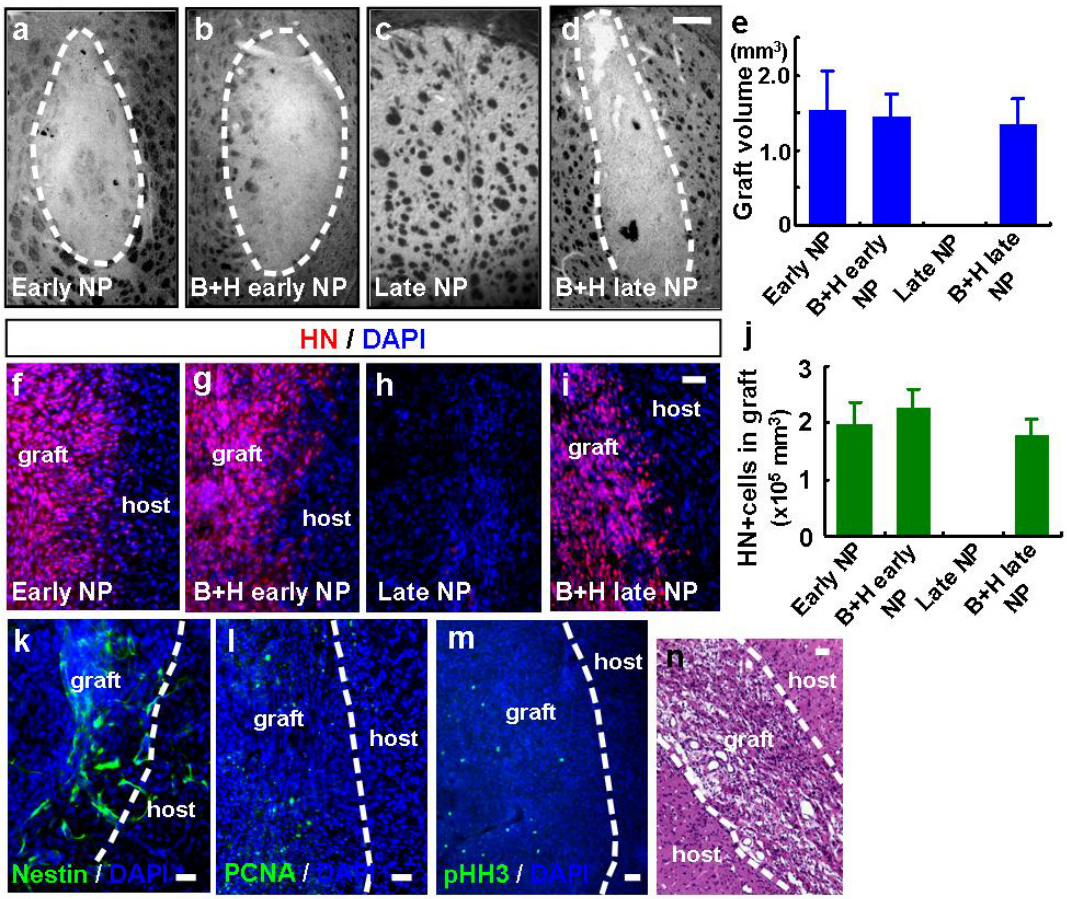
a
b
c
d
Early NP
B+H early NP
Late NP
B+H late NP
e
Graft volume (mm³)
2.0
1.0
0
Early NP
B+H early NP
Late NP
B+H late NP
HN / DAPI
f
g
h
i
graft
host
Early NP
B+H early NP
Late NP
B+H late NP
j
HN+cells in graft (x10⁵ mm³)
3
2
1
0
k
l
m
n
Nestin / DAPI
PCNA / DAPI
pHH3 / DAPI

Figure 15. Effect of Bcl-XL+SHH on *in vivo* survival of hES-NP cells. Cultures of hES-NP cells were prepared and transplanted to PD rats as described in 'Materials and Methods.' The animals were sacrificed 8 weeks after transplantation. Presented here are (a-d) representative light microscopic views of grafts in the striatum of PD rats transplanted with (a) naïve early NP (Early NP), (b) early NP transduced with Bcl-XL+SHH (B+H early NP), (c) late NP nontransduced (Late NP), and (d) B+H-transduced (B+H late NP) (scale bar, 200 μm); (e) the graft volume for each animal group; (f-i) immunofluorescent images for HN+ grafts (scale bar, 40 μm); (j) graph showing total numbers of HN+ cells in the grafts of the animals; (k-m), representative images for (k) cells positive for Nestin/DAPI, (l) PCNA/DAPI, and (m) pHH3/DAPI in the rats transplanted with B+H early NP; and (n) representative microscopic image of H&E-stained graft of early NP B+H. Dashed lines mark the borders of the grafts (scale bar 40 μm).

in vivo (Fig. 15d, e, I, j). Graft volumes (1.4±0.3 mm^3) and HN+ cells (492,596±243,097 cells) in animals grafted with B+H late NP cells were similar to those of animals grafted with early NP cells. These results show that B+H manipulation of late NP donor cells can completely prevent loss of viability post-transplantation.

The cells within grafts were morphologically uniform with no evidence of neoplastic change or tumor formation in H&E-stained tissues regardless of NP cell passage number and B+H transduction (Fig. 15n and data not shown). Although neural rosette structures did form in early NP cell cultures, the cells grafted did not generate neural rosettes by 8 weeks after transplantation. Subpopulations, however, were positive for the neural precursor cell marker nestin and the proliferating cell markers PCNA and pHH3 in all the grafts generated by early and late NP cells (Fig. 15k-m). Transduction with B+H did not significantly affect those immunoreactive cell populations or the shape of the resulting graft.

F. Optimal immunohistochemical detection of TH+ DA neurons in grafts of hES-NP cells

Most previous studies of hES cell-based transplantation in PD reported unexpectedly low yields of TH+ DA neurons in the grafts.[10,13,57,58] These low yields of hES cell-derived DA neurons *in vivo* contrast clearly with findings of viable DA neurons in abundance in brain grafts of mouse ES (mES)-derived NP cells.[59-61] Human DA neurons are more vulnerable to oxygen free radicals produced by TH enzyme activity than rodent DA neurons, and may therefore maintain only low levels of TH expression.[62,63] For this reason, the low DA neuron numbers in the transplants of hES-derived cells may be due to inefficient detection of TH antigenic determinants. We thus

varied the conditions of TH immunofluorescent staining in an effort to optimize results. Among the antibodies tested, TH antibody from Pel-freeze™ (see Materials and Methods) showed the highest sensitivity to hES-derived DA neurons in the grafts, giving the strongest positive signals under all conditions tested (data not shown). Inclusion of biotin-streptavidin amplification step,[64] modifications in the composition of blocking solution, fixative, and incubation time with the primary TH antibody had no apparent effect on the staining. However, antigen retrieval by SDS treatment (see Materials & Methods) greatly improved the TH-sensitivity of immunohistochemical detection of hES-DA neurons *in vivo* (Fig. 16a-d). Using the SDS method, we detected approximately 9-fold more TH+ cells, with stronger intensity of the positive signals, than without the treatment (131±34 cells/graft without, 1,262±207 cells/graft with SDS treatment; Fig. 16d, $n = 3$ grafts for each value; $p < 0.01$). The boiling method for antigen retrieval (see Materials & Methods) also enhanced TH+ signal intensity and the number of TH+ cells detected, but did not increase detection sensitivity to the degree that the SDS treatment did. The increased detection sensitivity with SDS treatment was further confirmed by comparing TH+ cell numbers in identical sections (Fig. 16e-g). We therefore used the SDS antigen retrieval method for all TH staining of sectioned tissues in this study.

G. TH+ DA neuron yield and behavioral assessment of PD rats grafted with hES-NP cells

In the animals with grafts of early NP cells, grafts showed an average of 976±366 TH+ cells (Fig. 17a, i), approximately five times the number we previously detected in hES-NP cell transplants without using the SDS treatment. Transplanting early NP cells transduced with Bcl-XL+SHH produced a similar yield of TH+ cells (1,140±276 cells;

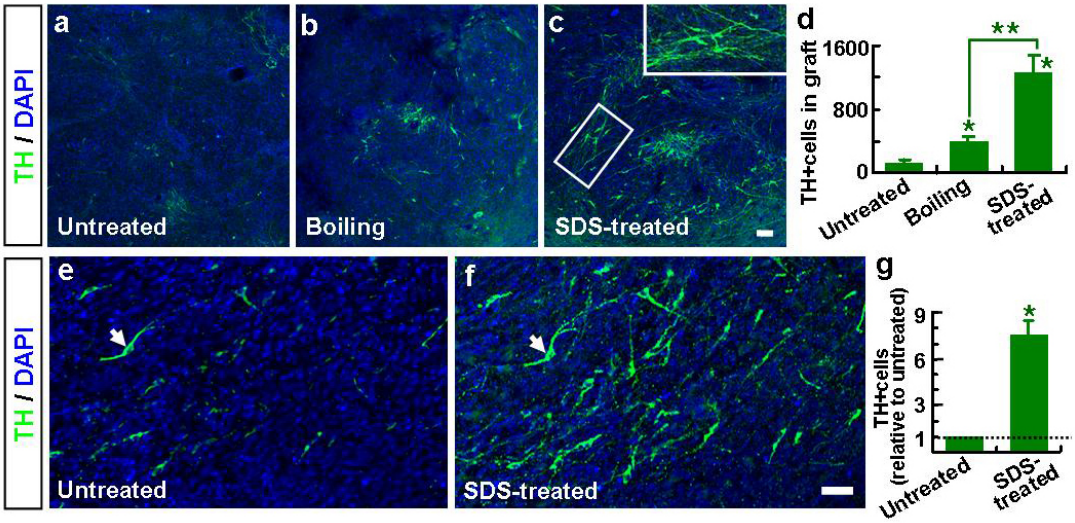
TH / DAPI
a
Untreated
b
Boiling
c
SDS-treated
d
TH+cells in graft
1600
800
0
**
*
*
Untreated
Boiling
SDS-treated
TH / DAPI
e
Untreated
f
SDS-treated
g
TH+cells (relative to untreated)
9
6
3
1
*
Untreated
SDS-treated

Figure 16. Antigen retrieval improves the sensitivity of TH immunohistochemical detection for DA neurons in hES-NP-derived grafts. Comparison of TH+ cell numbers detected without (a) and with antigen retrieval using the boiling method (b) or SDS treatment (c) in adjacent sections of the same graft. Eight weeks after transplantation, brain slices from three rats grafted with B+H late NP cells were prepared. Shown in (a-c) are representative images for TH+ cells in the grafts obtained from adjacent sections with the different methods. Inset: high-powered view of the boxed area. Graph (d) depicts the average TH+ cell numbers of 3 grafts calculated as described in 'Materials and Methods'. Significantly different from *untreated and ** boiling method at $p < 0.01$, n=3. (e-g), comparison of TH+ cell detection sensitivity between control (no treatment) and SDS-treated methods in identical sections. Ten sections (each derived from different animals) were initially subjected to TH immunostaining without antigen retrieval, and TH-stained cells per section counted. Subsequently, identical sections were carefully washed and stained with SDS, and TH+ cells counted. Shown in (e) and (f), respectively, are images for TH+ cells stained with untreated and SDS-treated methods in an identical section. Arrows indicate an identical TH+ cell in the images. Graph (g) represents the relative values of TH+ cells to those of control untreated cells. *Statistical comparisons were made between TH+ cell numbers detected with the two methods in each identical section using the paired t-test (n= 10, t= -2.716, p=0.024). Scale bars, 20 um.

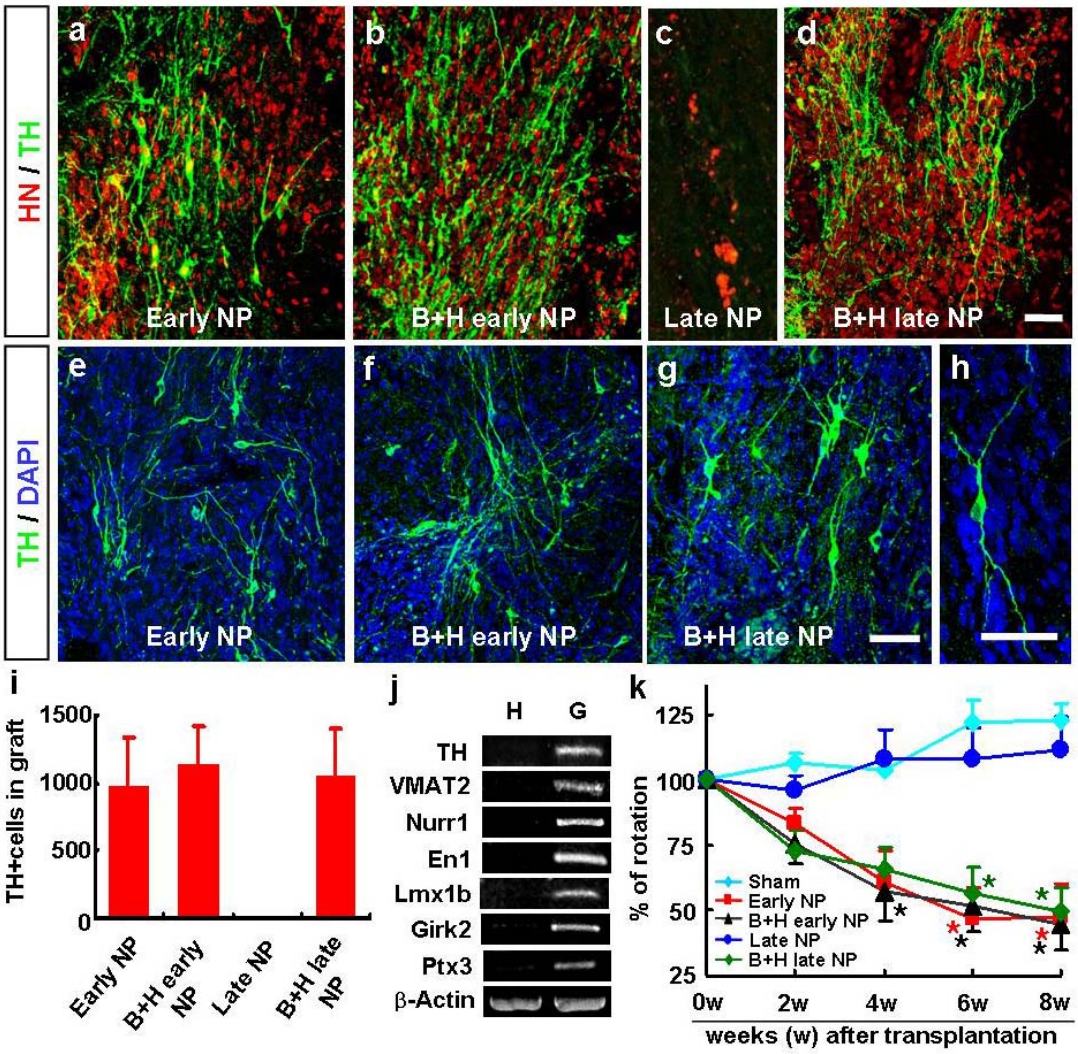
HN / TH
TH / DAPI
a
b
c
d
e
f
g
h
Early NP
B+H early NP
Late NP
B+H late NP
i
TH+cells in graft
1500
1000
500
0
Early NP
B+H early NP
Late NP
B+H late NP
j
H
G
TH
VMAT2
Nurr1
En1
Lmx1b
Girk2
Ptx3
β-Actin
k
% of rotation
125
100
75
50
25
Sham
Early NP
B+H early NP
Late NP
B+H late NP
0w
2w
4w
6w
8w
weeks (w) after transplantation

Figure 17. In vivo analyses of hES-NP cells transplanted to PD rats. hES-NP cells at different NP passage numbers with or without B+H transduction were prepared and injected into PD rats as described. (a-i), DA neuron yields from hES-NP cells transplanted into PD rats. Immunostaining for TH was performed using the SDS antigen retrieval method as described. For TH/HN-double immunostaining (a-d), the tissue sections were initially stained with HN without SDS treatment, followed by TH-staining with SDS-treatment. The TH and TH/HN images were obtained by stacking z-series through the thickness of the section (35 μm). Shown in (a-h) are confocal microscopic images of TH+/HN+ (a-d) and TH+ (e-h) cells in the striatum of rats grafted with the indicated hES-NP cells. Panel (h) is an image from an isolated TH-stained DA cell with well-defined neurite outgrowths obtained from a graft of hES-NP at P2. Scale bars, 40 μm. Graph (i) depicts total numbers of TH+ cells in the grafts of the animals. j, Midbrain DA neuron marker expression in hES-NP cell grafts. After transplantation with B+H-transduced NP-P9, RNA samples were prepared from ipsilateral graft (G) and contralateral host striatum (H). RT-PCR analysis of markers specific for general (TH, VMAT2) and midbrain-type (Nurr1, En1, Lmx1b, Girk2, Ptx3) DA neurons. k, amphetamine-induced rotation test. For the sham control, five animals were injected with PBS by the same schedule as the cell-grafted animals. Each value depicts mean ± SEM of % changes in rotation scores as compared to pre-transplantation values. Statistical comparisons were made by ANOVA, followed by the Scheffe test. * <0.05 from PBS-injected group, n=9 (Early NP), n=16 (B+H early NP), n=7 (Late NP), and n=16 (B+H late NP).

Fig. 17b, i). In rats that received non-transduced late NP cells, we detected neither HN+ graft formation (Fig. 15h, j) nor TH+ graft formation (Fig. 17c, i). However, the numbers of TH+ cells in rats grafted with B+H late NP cells were similar to the numbers in grafts of early NP cells (1,056±342 cells, Fig. 17d, i). The TH+ cells in grafts were morphologically mature, with extensive neurite outgrowth (Insets of Fig. 16c and 17e-h) and abundant expression of the midbrain DA neuronal markers was detected in hES-NP-derived grafts (Fig. 17j).

Consistent with the TH+ cell numbers and morphological maturity in the transplants, animals grafted with early NP cells showed significant reductions in amphetamine-induced rotation scores in 8 weeks after transplantation (Fig. 17k). Compared with pre-transplantation values, the rotation scores at 8 weeks were 47±13% ($p < 0.05$) for early NP transplants and 45±10% ($p < 0.05$) for those with B+H early NP cells. None of the animals grafted with non-transduced late NP cells showed a reduction in the rotation score. Average amphetamine-induced rotations at 8 weeks increased relative to pre-implantation values in these animals (111±6%). By contrast, 8 of 16 rats grafted with B+H-transduced late NP cells showed reductions in rotation scores of more than 50%. Average rotation score in animals with B+H late NP transplants was 50±9% ($p < 0.05$) of the pre-implantation value at 8 weeks after transplantation. The rotation results were also expressed as the numbers of turns per hour Fig. 18. These data indicate that manipulation of Bcl-XL and SHH genes together may overcome the loss of viability and functional activity of late hES-NP cells in transplants to PD rats.

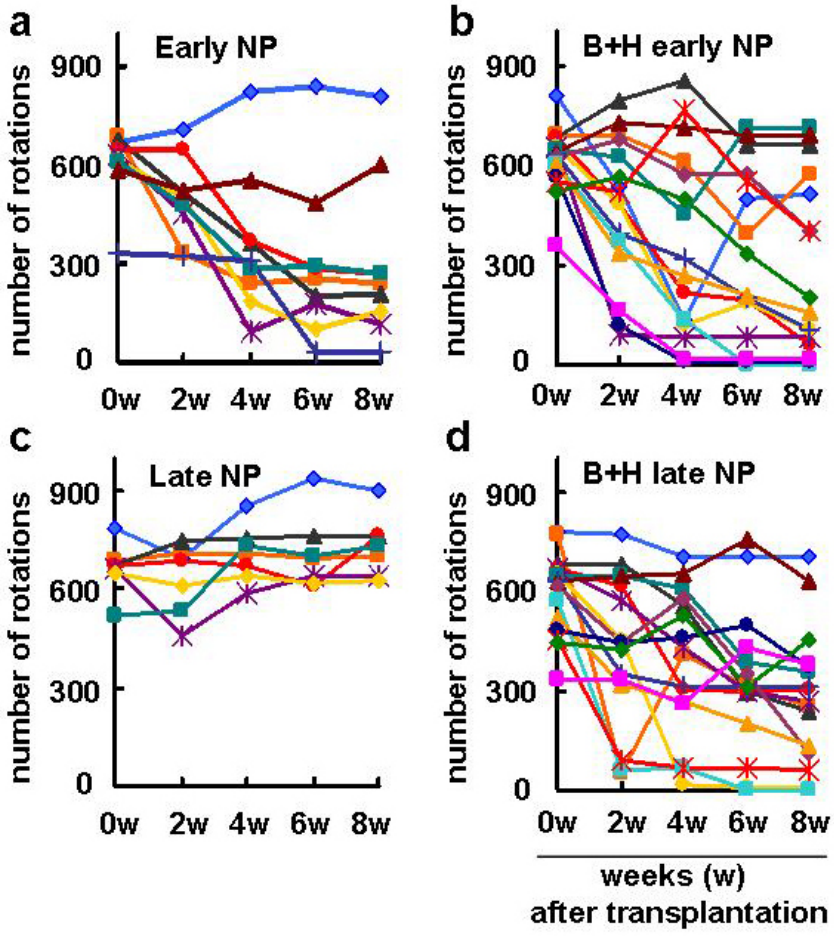

Figure 18. Amphetamine-induced rotation scores for 1 h obtained from individual animals transplanted with early NP (a), B+H early NP (b), late NP (c) and B+H late NP (d).

IV. DISCUSSION

The present study demonstrates that NP cells derived from hES cells were expanded 2×10^4-fold during 6 passages over >1 month, without losing their differentiation potentials toward an enriched population of DA neurons, which exhibited functionalities as a pre-synaptic DA neuron. Furthermore, we further passaged HSF-6 hES-NP cells up to 12 NP passages, and observed that the proliferative and enriched DA neuron yields of the longer-passaged hES-NP cells were, at least, unaltered (data not shwon). Thus it is undetermined yet how much longer the cellular properties of hES-NP could be maintained by *in vitro* culture. Such long-term maintenance of proliferative and developmental capacity of cultured precursors is quite exceptional, considering that culture period-dependent alteration in cellular properties is a rather general finding in cultures of stem or precursor cells derived from specific brain tissues. Specifically, neural precursor cells derived from the ventral mesencephalons of rat embryonic brains were expanded only 1,000-[34] or 5,400-fold[33] in cell numbers and almost completely lost their potential to differentiate into TH+ neurons after 4 weeks of *in vitro* culture.[33,34,65] In addition, the neurogenic differentiation potential of neural precursors derived from embryonic brain switches to an astrocytic one during *in vitro* cultures.[32] Thus, maintenance of the ratio of neuron/astrocyte cell number in differentiated cultures for hES-NP cells (Fig. 6g) is another contrasting finding between hES-NP cells and embryonic brain-derived NP cells. Similar to our findings, a recent study demonstrated that NP cells derived from mouse ES cells efficiently yielded DA cells after 4 weeks of *in vitro* expansion.[34] Thus, *in vitro* maintenance of precursor cell properties seems to be specific to NP cells derived from ES cells. As a possible explanation for the ES-derived

NP cell properties, it is suggested that NP cells generated from ES cells *in vitro* are early in the developmental process (such as primitive neuroepithelial cells), and the maturation process of the early NP cells into later cells is retarded under *in vitro* culture conditions.[66] This is probably because of the lack of *in vivo* environmental factors required for the maturation process, such as paracrine signals derived from blood vessels of endothelial cells.[67]

In this study, we have also shown that extended passage of these NP cells depletes neuroepithelial rosette structures, and may thereby contribute to a decrease in their tumorigenic potential after transplantation. The extended cell expansion period with multiple passages also resulted in a significant reduction in the percentage of Oct3/4+ undifferentiated hES cells during expansion, although the subculture procedures could not completely eliminate undifferentiated cells. These findings suggest a substantial possibility of teratoma formation after hES-NP cell transplantation. However, consistent with previous reports[57,48,68], none of the animals grafted with our hES-NP cells showed overt tumor formation for at least 2 months after transplantation. A plausible explanation for the absence of teratoma formation after transplantation of hES-NP cells is our interesting observation that the survival of Oct3/4+ cells in hES-NP cell cultures was absolutely dependent on bFGF supplementation; undifferentiated cells were completely eliminated by simply culturing for several days in bFGF-free media. Because the transplanted brains surely do not provide a bFGF-enriched environment, any undifferentiated cells that were injected should not survive in the host brains. This finding suggests that the possibility of teratoma formation after transplantation of hES-NP cells might be lower than expected based on the number of Oct3/4+ cells present in the hES-NP donor cell solution. However, at the clinical level, donor cell preparation requires

steps capable of completely eliminating undifferentiated cells. As indicated, pre-culturing hES-NP cells in bFGF-free media for several days before transplantation might be a simple practical way to generate donor NP cells for clinical applications.

Cell viability steadily declined with passage, however, and virtually none of the late NP cells survived in a graft (Fig. 12 and 15 h, j). We then showed that transgenic expression of Bcl-XL and SHH in hES-NP cells additively enhances their survival and prevents depletion of late NP cells in brain transplants *in vivo* (Fig. 14 and 15 i, j). In addition to its anti-apoptotic role, Bcl-XL participates at various stages of neuronal differentiation, including cell fate determination,[69,70] maturation, and acquisition of functional properties in cultures of rodent neurons.[71,72] In mouse-derived embryonic stem (mES) cells, the overexpression of Bcl-XL enhances the generation and maturation of DA neurons and the development of dopaminergic activity.[61] SHH is a signaling factor that emanates from the floor plate of the developing brain. This secreted molecule continues to be expressed in the adult brain, where it plays a role in promoting the survival[73] and proliferation[74] of neural precursor cells. The SHH-mediated ventralizing effect in the developing brain is associated with induction of DA neuronal-fate determination in early embryonic midbrain precursors.[42,75] Consistent with this observation, SHH cytokine treatment in mES-derived NP cells has been shown to enhance the yield of DA neurons in culture.[43] By contrast, neither Bcl-XL nor SHH showed similar effects on neuronal or DA neuronal differentiation in hES-NP cultures. Further study may reveal mechanisms for the species-dependent differences of the cytokine effects.

Most investigators report detection of no or very few (0-400) TH+ cells *in vivo* after transplanting hES cell-derivatives.[10,13,57,58,76] Similarly, transplantation of MESC2.10 cells from a human mesencephalic cell line did not generate TH+ cells in the striatum of PD

rats even though the cells exhibit features of DA neurons *in vitro*.[77] This contrasts sharply with the enrichment of TH+ DA neurons in the brains of PD rats receiving mES-derived NP cells[59-60] or rat embryonic midbrain cells directly.[52] The DA neuron yields in transplants may therefore represent an important distinction between human DA neurons and those of rodents. There are several possible causes for the poor DA neuron yields in the grafts generated by human cells. Similar to our findings here (Fig. 13), Paul et al. found that TH expression in human DA cells disappears in a medium lacking differentiation factors (i.e., cAMP and neurotrophins),[77] but could be restored by repletion of those factors, indicating unstable TH expression of human DA cells depending on the trophic factors. Thus, the trophic factor dependency of human cells in their TH expression may be a prime cause for the relatively few TH+ cells in the human neuronal transplants, because enrichment of these trophic supports cannot be expected in the host environment. Second, low TH+ cells of human cell transplants may stem from suboptimal conditions for immunohistochemical detection of TH in previous measurements, which would underestimate the numbers of human DA neurons in the grafts. We base this assertion on our experience and communications with others, having shown distinct differences between rodent and human cells with respect to antigenic properties and detection sensitivities for several DA neuronal markers. Detection sensitivity may be especially important, because these cells are extremely sensitive to oxidative injury and may normally maintain low levels of TH expression to minimize the oxidative stress imposed by TH activity.[62,63] As we show here, antigen retrieval with SDS treatment can significantly improve immunohistochemical sensitivity to TH determinants in human DA cells *in vivo*.

Given the restricted access to human tissues and cells, most investigators of midbrain dopaminergic function have used rodent models and DA cell lines. But while human and rodent midbrain DA neurons share many properties, they differ sharply in important ways, including midbrain marker gene expression and response to mitogens, differentiation factors, and conditions in their tissue environment. The need for neurological therapies grows, and with it, the need for experimental systems based on human cells. In this regard, our hES-NP cells provide a stable, renewable population for studies of human dopaminergic function and optimization of a cell therapy for PD.

V. CONCLUSION

In conclusion, this study established that hES-derived NP cells maintain their proliferative capacity and dopaminergic phenotype through multiple cell passages, through expansion, this cell type can generate the large, stable, homogeneous populations required for transplantation therapy of PD. We have shown that extended passage of these NP cells depletes neuroepithelial rosette structures, and may thereby contribute to a decrease in their tumorigenic potential after transplantation. In this regard, our hES-NP cells provide a stable, renewable population for studies of human dopaminergic function and optimization of cell therapy for PD.

REFERENCES

1. Freed CR, Greene PE, Breeze RE, Tsai WY, DuMouchel W, Kao R, et al. Transplantation of embryonic dopamine neurons for severe Parkinson's disease. The New England Journal of Medicine 2001;344:710-9.
2. Olanow CW, Goetz CG, Kordower JH, Stoessl AJ, Sossi V, Brin MF, et al. A double-blind controlled trial of bilateral fetal nigral transplantation in Parkinson's disease. Ann Neurol 2003;54:403-14.
3. Snyder BJ, Olanow CW. Stem cell treatment for Parkinson's disease: an update for 2005. Curr Opin Neurol 2005;18:376-85.
4. Amit M, Carpenter MK, Inokuma MS, Chiu CP, Harris CP, Waknitz MA, et al. Clonally derived human embryonic stem cell lines maintain pluripotency and proliferative potential for prolonged periods of culture. Dev Biol 2000;227:271-8.
5. Reubinoff BE, Pera MF, Fong CY, Trounson A, Bongso A. Embryonic stem cell lines from human blastocysts: somatic differentiation *in vitro*. Nat Biotechnol 2000;18:399-404.
6. Thomson JA, Itskovitz-Eldor J, Shapiro SS, Waknitz MA, Swiergiel JJ, Marshall VS, et al. Embryonic stem cell lines derived from human blastocysts. Science 1998;282:1145-7.
7. Draper JS, Smith K, Gokhale P, Moore HD, Maltby E, Johnson J, et al. Recurrent gain of chromosomes 17q and 12 in cultured human embryonic stem cells. Nat Biotechnol 2004;22:53-4.

8. Imreh MP, Gertow K, Cedervall J, Unger C, Holmberg K, Szoke K., et al. *In vitro* culture conditions favoring selection of chromosomal abnormalities in human ES cells. J Cell Biochem 2006;99:508-16.

9. Maitra A, Arking DE, Shivapurkar N, Ikeda M, Stastny V, Kassauei K, et al. Genomic alterations in cultured human embryonic stem cells. Nat Genet 2005;37:1099-103.

10. Brederlau A, Correia AS, Anisimov SV, Elmi M, Roybon L, Paul G, et al. Transplantation of human embryonic stem cell-derived cells to a rat model of Parkinson's disease: effect of *in vitro* differentiation on graft survival and teratoma formation. Stem Cells 2006;24:1433-40.

11. Schulz TC, Noggle SA, Palmarini GM, Weiler DA, Lyons IG, Pensa KA, et al. Differentiation of human embryonic stem cells to dopaminergic neurons in serum-free suspension culture. Stem Cells 2004;22:1218-38.

12. Zeng X, Cai J, Chen J, Luo Y, You ZB, Fotter E, et al. Dopaminergic Differentiation of Human Embryonic Stem Cells. Stem Cells 2004;22:925-40.

13. Park CH, Minn YK, Lee JY, Choi DH, Chang MY, Shim JW, et al. *In vitro* and *in vivo* analyses of human embryonic stem cell-derived dopamine neurons. J Neurochem 2005;92:1265-76.

14. Perrier AL, Tabar V, Barberi T, Rubio ME, Bruses J, Topf N, *et al*. Derivation of midbrain dopamine neurons from human embryonic stem cells. Proc Natl Acad Sci USA 2004;101:12543-8.

15. Okabe S, Forsberg-Nilsson K, Spiro AC, Segal M, McKay RD. Development of neuronal precursor cells and functional postmitotic neurons from embryonic stem cells *in vitro*. Mech Dev 1996;59:89-102.

16. Kim JY, Koh HC, Lee JY, Chang MY, Kim YC, Chung HY, et al. Dopaminergic neuronal differentiation from rat embryonic neural precursors by Nurr1 overexpression. J Neurochem 2003;85:1443-54.

17. Soltys BJ, Gupta RS. Interrelationships of endoplasmic reticulum, mitochondria, intermediate filaments, and microtubules - a quadruple fluorescence labeling study. Biochem Cell Biol 1992;70:1174-86.

18. Brown D, Lydon J, McLaughlin M, Stuart-Tilley A, Tyszkowski R, Alper S. Antigen retrieval in cryostat tissue sections and cultured cells by treatment with sodium dodecyl sulfate (SDS). Histochem Cell Biol 1996;105:261-7.

19. Wilson III DM, Bianchi C. Improved immunodetection of nuclear antigens after sodium dodecyl sulfate treatment of formaldehyde-fixed cells. J Histochem Cytochem 1999;47:1095-100.

20. Shi SR, Key ME, Kalra KL. Antigen retrieval in formalin-fixed paraffin-embedded tissues: an enhancement method for immunohistochemical staining based on microwave oven heating of tissue sections. J Histochem Cytochem 1991;39:741-8.

21. Cattoretti G, Pilere S, Parravicini C, Becker MHG, Poggi S, Bifulco C, et al. Antigen unmasking on formalin-fixed, paraffin-embedded tissue sections. J Pathol 1993;171:83-98.

22. Jiao,Y, Sun Z, Lee T, Fusco FR, Kimble TD, Meade CA, et al. A simple and sensitive antigen retrieval method for free-floating and slide-mounted tissue sections. J Neurosci Methods 1999;93:149-62.

23. Abercrombie M. Estimation of nuclear populations from microtome sections. Anat Rec 1946;94:239-47.

24. Shim JW, Koh HC, Chang MY, Roh E, Choi CY, Oh, YJ et al. Enhanced *in vitro* midbrain dopamine neuron differentiation, dopaminergic function, neurite outgrowth, and 1-methyl-4-phenylpyridium resistance in mouse embryonic stem cells overexpressing Bcl-XL. J Neurosci 2004;24:843-52.

25. Joyner AL. Engrailed, Wnt and Pax genes regulate midbrain-hinbrain development. Trends Genet 1996;12:15-20.

26. Bird JM, Kimber SJ. Oligosaccharides containing fucose linked alpha(1-3) and alpha(1-4) to N-acetylglucosamine cause decompaction of mouse morulae. Dev Biol 1984;104:449-60.

27. Capela A, Temple S. LeX/ssea-1 is expressed by adult mouse CNS stem cells, identifying them as noependymal. Neuron 2002;35:865-75.

28. Capela A, Temple, S. LeX is expressed by principle progenitor cells in the embryonic nervous system, is secreted into their environment and binds Wnt-1. *Dev Biol* 2006;291:300-13.

29. Bayer SA, Altman, J. Neurocortical development (NY); Raven Press; 1991.

30. Jacobson M. Developmental Neurobiology (NY); Plenum Press; 1991.

31. Qian X, Shen O, Goderia SK, He W, Capela A, Davis AA, et al. Timing of CNS cell generation: a programmed sequence of neuron and glial cell production from isolated murine cortical stem cells. Neuron 2000;28:69-80.

32. Chang MY, Park CH, Lee SY, Lee SH. Properties of cortical precursor cells cultured long term are similar to those of precursors at later developmental stages. Dev Br Res 2004;153:89-96.

33. Yan J, Studer L, McKay RD. Ascorbic acid increases the yield of dopaminergic neurons derived from basic fibroblast growth factor expanded mesencephalic precursors. J Neurochem 2001;76:307-11.

34. Chung S, Shin BS, Hwang M, Lardaro T, Kang UJ, Isacson O, et al. Neural precursors derived from embryonic stem cells, but not those from fetal ventral mesencephalon, maintain the potential to differentiate into dopaminergic neurons after expansion *in vitro*. Stem Cells 2006;24:1583-93.

35. Yamada T, McGeer PL, Baimbridge KG, McGeer EG. Relative sparing in Parkinson's disease of substantia nigra dopamine neurons containing calbindin-D28K. Brain Res 1990;256:303-7.

36. Gaspar P, Ben Jelloun N, Febvret A. Sparing of the dopaminergic neurons containing calbindin-D28k and of the dopaminergic mesocortical projections in weaver mutant mice. J Neurosci 1994;61:293-305.

37. Damier P, Hirsch EC, Agid Y, Graybiel AM. The substantia nigra of the human brain. I. Nigrosomes and the nigral matrix, a compartmental organization based on calbindin D(28K) immunohistochemistry. Brain 1999;122:1421-36.

38. Mendez I, Sanchez-Pernaute R, Cooper O, Viñuela A, Ferrari D, Bjo¨rklund L, et al. Cell type analysis of functional fetal dopamine cell suspension transplants in the striatum and substantia nigra of patients with Parkinson's disease. Brain 2005;128:1498-510.

39. Thompson L, Barraud P, Andersson E, Kirik D, Bjorklund A. Identification of dopaminergic neurons of nigral and ventral tegmental area subtypes in grafts of fetal ventral mesencephalon based on cell morphology, protein expression, and efferent projections. J Neurosci 2005;25:6467-77.

40. McRitchie DA, Hardman CD, Halliday GM. Cytoarchitectural distribution of calcium binding proteins in midbrain dopaminergic regions of rats and humans. J Comp Neurol 1996;364:121-50.

41. Roy NS, Cleren C, Singh SK, Yang L, Beal MF, Goldman SA. Functional engraftment of human ES cell-derived dopaminergic neurons enriched by coculture with telomerase-immortalized midbrain astrocytes. Nat Med 2006;12:1259-68.

42. Ye W, Shimamura K, Rubenstein JLR, Hynes M, Rosenthal A. FGF and *Shh* signals control dopaminergic and serotonergic cell fate in the anterior neural plate. Cell 1998;93:755-66.

43. Lee SH, Lumelsky N, Studer L, Auerbach JM, McKay RD. Efficient generation of midbrain and hindbrain neurons from mouse embryonic stem cells. Nat Biotechnol 2000;18:675-9.

44. Gall CM, Hendry SH, Seroogy KB, JonesEG, Haycock JW. Evidence for coexistence of GABA and dopamine in neurons of the rat olfactory bulb. J Comp Neurol 1987;266:307-18.

45. Max SR, Bossio A, Iacovitti L. Co-expression of tyrosine hydroxylase and glutamic acid decarboxylase in dopamine differentiation factor-treated striatal neurons in culture. Dev Brain Res 1996;91:140-2.

46. Elkabetz Y, Panagiotakos G, Al Shamy G, Socci ND, Tabar V, Studer L. Human ES cell-derived neural rosettes reveal a functionally distinct early neural stem cell stage. Genes Dev 2008;22: 152-65.

47. Sonntag KC, Pruszak J, Yoshizaki T, van Arensbergen J, Sanchez-Pernaute R, Isacson O. Enhanced yield of neuroepothelial precursors and midbrain-like

dopaminergic neurons from human embryonic stem cells using the bone morphogenic protein antagonist noggin. Stem Cells 2007;25:411-8.

48. Yang D, Zhang ZJ, Oldenburg M, Ayala M, Zhang SC. Human embryonic stem cell-derived dopaminergic neurons reverse functional deficit in parkinsonian rats. Stem Cells 2008;26:55-63.

49. Hong S, Kang UJ, Isacson O, Kim KS. Neural precursors derived from human embryonic stem cells maintain long-term proliferation without losing the potential to differentiate into all three neural lineages, including dopaminergic neurons. J Neurochem 2008;104:316-24.

50. Hyman C, Hofer M, Barde YA, Juhasz M, Yancopoulos GD, Squinto SP, et al. BDNF is a neurotrophic factor for dopaminergic neurons of the substantia nigra. Nature 1991;350:230-32.

51. Lin LF, Doherty DH, Lile JD, Bektesh S, Collins F. GDNF: a glial cell line-derived neurotrophic factor for midbrain dopaminergic neurons. Science 1993;260:1130-2.

52. Studer L, Tabar V, Mckay RD. Transplantation of expanded mesencephalic precursors leads to recovery in parkinsonian rats. Nat Neurosci 1998;1:290-5.

53. Xiao H, Hirata Y, Isobe K, Kiuchi K. Glial cell line-derived neurotrophic factor up-regulates the expression of tyrosine hydroxylase gene in human neuroblastoma cell lines. J Neurochem 2002;82:801-8.

54. Yuan J, Yankner BA. Apoptosis in the nervous system. Nature 2000;407:802-9.

55. Thibert C, Teillet MA, Lapointe F, Mazelin L, Le Douarin NM, Mehlen P. Inhibition of neuroepithelial patched-induced apoptosis by sonic hedgehog. Science 2003;301:843-6.

56. Miao N, Wang M, Ott JA, D'Alessandro JS, Woolf TM, Bumcrot DA, et al. Sonic hedgehog promotes the survival of specific CNS neuron populations and protects these cells from toxic insult *in vitro*. J Neurosci 1997;17:5891-9.

57. Ben-Hur T, Idelson M, Khaner H, Pera M, Reinhartz E, Itzik A, et al. Transplantation of human embryonic stem cell-derived neural progenitors improves behavioral deficit in Parkinsonian rats. Stem Cells 2004;22:1246-55.

58. Martinat C, Bacci JJ, Leete T, Kim J, Vanti WB, Newman AH, et al. Cooperative transcription activation by Nurr1 and Pitx3 induces embryonic stem cell maturation to the midbrain dopamine neuron phenotype. Proc Natl Acad Sci USA 2006;103:2876-9.

59. Bjorklund LM, Sanchez-Pernaute R, Chung S, Andersson T, Chen IY, McNaught KS, et al. Embryonic stem cells develop into functional dopaminergic neurons after transplantation in a Parkinson rat model. Proc Natl Acad Sci USA 2002;99:2344-9.

60. Kim JH, Auerbach JM, Rodrı´guez-Go´mez JA, Velasco I, Gavin D, Lumelsky N, et al. Dopamine neurons derived from embryonic stem cells function in an animal model of Parkinson's disease. Nature 2002;418:50-6.

61. Shim JW, Koh HC, Chang MY, Roh E, Choi CY, Oh YJ, et al. Enhanced *in vitro* midbrain dopamine neuron differentiation, dopaminergic function, neurite outgrowth, and 1-methyl-4-phenylpyridium resistance in mouse embryonic stem cells overexpressing Bcl-XL. J Neurosci 2004;24:843-52.

62. Liste I, Garcia-Garcia E, Martinez-Serrano A. The generation of dopaminergic neurons by human neural stem cells is enhanced by Bcl-XL, both *in vitro* and *in vivo*. J Neurosci 2004a;24:10786-95.

63. Liste I, Navarro B, Johansen J, Bueno C, Villa A, Johansen TE, et al. Low-level tyrosine hydroxylase (TH) expression allows for the generation of stable TH+ cell lines of human neural stem cells. Hum Gene Ther 2004b;15:13-20.

64. Guesdon JL, Ternynck T, Avrameas S. The use of avidin-biotin interaction in immunoenzymatic techniques. J Histochem Cytochem 1979;27:1131-9.

65. Ko JY, Lee JY, Park CH, Lee SH. Effect of cell-density on *in vitro* dopaminergic differentiation of mesencephalic precursor cells. Neuroreport 2005;16:499-503.

66. Hitoshi S, Seaberg RM, Koscik C, Alexson T, Kusunoki S, Kanazawa I, et al. Primitive neural stem cells from the mammalian epiblast differentiate to definitive neural stem cells under the control of Notch signaling. Genes Dev 2004;18:1806-11.

67. Shen Q, Goderie SK, Jin L, Karanth N, Sun Y, Abramova N, et al. Endothelial cells stimulate self-renewal and expand neurogenesis of neural stem cells. Science 2004;304:1338-40.

68. Chiba S, Lee YM, Zhou W, Freed CR. Noggin enhances dopamine neuron production from human embryonic stem cells and improves behavioral outcome after transplantation into Parkinsonian rats. Stem Cells 2008;26:2810-20.

69. Chang MY, Sun W, Ochiai W, Nakashima K, Kim SY, Park CH, et al. Bcl-XL/Bax proteins direct the fate of embryonic cortical precursor cells. Mol Cell Biol 2007;27:4293-305.

70. Liste I, Garcia-Garcia E, Bueno C, Martinez-Serrano A. Bcl-XL modulates the differentiation of immortalized human neural stem cells. Cell Death Differ 2007;14:1880-92.

71. Park CH, Kang JS, Shin YH, Chang MY, Chung S, Koh HC, et al. Acquisition of *in vitro* and *in vivo* functionality of Nurr1-induced dopamine neurons. FASEB J 2006;20:2553-5.

72. Jonas EA, Hoit D, Hickman JA, Brandt TA, Polster BM, Fannjiang Y, et al. Modulation of synaptic transmission by the BCL-2 family protein BCL-xL. J Neurosci 2003;23:8423-31.

73. Machold R, Hayashi S, Rutlin M, Muzumdar MD, Nery S, Corbin JG, et al. Sonic hedgehog is required for progenitor cell maintenance in telencephalic stem cell niches. Neuron 2003;39:937-50.

74. Lai K, Kaspar BK, Gage FH, Schaffer DV. Sonic hedgehog regulates adult neural progenitor proliferation *in vitro* and *in vivo*. Nat Neurosci 2003;6:21-7.

75. Andersson E, Tryggvason U, Deng Q, Friling S, Alekseenko Z, Robert B, et al. Identification of intrinsic determinants of midbrain dopamine neurons. Cell 2006;124:393-405.

76. Zeng X, Cai J, Chen J, Luo Y, You ZB, Fotter E, et al. Dopaminergic Differentiation of Human Embryonic Stem Cells. Stem Cells 2004;22:925-40.

77. Paul G, Christophersen NS, Raymon H, Kiaer C, Smith R, Brundin P. Tyrosine hydroxylase expression is unstable in a human immortalized mesencephalic cell line – Studies *in vitro* and after intracerebral grafting *in vivo*. Mol Cell Neurosci 2007;34:390-9.

인간 배아줄기세포로부터 신경전구세포 및 도파민 신경세포의 효율적 분화 및 파킨슨병 동물 모델에의 적용

<지도교수 : 김 동 욱>

연세대학교 대학원 의과학과

고 지 윤

인간 배아줄기세포는 매우 많은 양의 도파민 신경세포를 지속적으로 만들어 내는 배쪽(ventral) 중뇌형 신경전구세포(neural precursor cells)로 분화 유도될 수 있다. 이 결과는 인간배아줄기세포로부터 유래된 신경전구세포가 파킨슨병의 치료를 위한 세포 대체 전략으로 사용될 수 있는 유용한 세포 공급원이 될 수 있음을 시사한다. 이러한 기대를 보다 분명하게 하기 위하여, 본 연구에서는 인간 배아줄기세포로부터 유래된 신경전구세포의 특성을 (1) 대규모로 인간 도파민 신경세포를 안정하게 공급할 수 있는 신경전구세포의 능력과 (2) 효과적이고 안전한 세포 치료를 위해 대단히 중요한 문제인 세포 생존 및 암 발생 가능성의 두 관점에서 면밀히 조사하였다.

우선, 본 연구에서는 인간 배아줄기세포로부터 유래된 신경전구세포가 기능 분석 및 치료적 이용을 위하여 인간 도파민 신경세포를 대규모 생산할

잠재성이 있는지 확인하였다. 이 같은 가능성을 검증하기 위하여, 본 연구에서는 인간줄기세포 유래 신경전구세포를 시험관 내에서 1.5 개월 동안 6 차례 계대로 확장하였고, 전 신경전구세포 계대에 걸쳐 증식 및 분화 특성을 규명하였다. 흥미롭게도, 그 시험관 내(*in vitro*) 기간을 통해 표현형 유전자 발현의 변화 없이 전체 인간 배아줄기세포 유래 신경전구세포의 수가 2×10^4 배 증가하였다. 또한, 그 세포들은 시험관 내에서 도파민 신경세포 기능을 나타내는 신경세포로 분화하는 세포 자신의 능력을 그대로 유지하였다. 게다가, 인간 배아줄기세포 유래 신경줄기세포는 분화 및 발생 잠재성을 잃지 않고 동결 보관할 수 있었다. 이와 같은 결과는, 본 연구를 통해 확립된 인간 배아줄기세포유래 신경전구세포가 파킨슨병 세포 치료를 위한 안정적인 세포 공급원이 될 수 있음을 시사한다.

본 연구의 두번째 부분에서는 파킨슨병에 대한 세포 치료적 접근시 중요한 문제인 인간 배아줄기세포 유래 신경전구세포의 생존 및 암 발생 양상을 기술하였다. 이식후 종양을 발생하는 세포(구조)로 알려진 원시 신경상피세포 구조(neuroepithelial rosettes)와 Oct3/4 를 발현하는 미분화 배아줄기세포는 인간 배아줄기세포 유래 신경전구세포를 시험관 내에서 장기간 계대 배양시 사라지거나 줄어들며, 소량으로 남아있던 Oct3/4 발현 세포들도 분화를 유도하는 조건하에서 3-4 일 계대 배양함으로써 완전하게 제거할 수 있었다. 그러나 장기간 계대 배양한 인간 배아줄기세포유래 신경전구세포는 세포이식 후에 급격히 세포 사멸이 진행되었다. 이러한

이식후 세포 생존 문제는 본 연구에서 Bcl-XL 와 sonic hedgehog 를 과발현함으로써 완전히 해결되었으며, 장기간 계대 배양한 인간 배아줄기세포유래 신경전구세포에 Bcl-XL 와 sonic hedgehog 유전자를 도입함으로써 파킨슨병 세포 치료시 종양의 발생없이 세포 생존 증진을 도모할 수 있는 세포를 공급할 수 방안을 제시하였다.

결론적으로, 본 연구에서는 인간 배아줄기세포에서 유래된 신경줄기세포가 언제든지 도파민 신경세포를 안정하고 지속적으로 공급할 수 있는 세포 공급원으로 이용될 수 있다는 증거를 제공하였으며, 이러한 신경전구세포의 계속된 계대 배양은 암 발생 가능성으로부터 벗어난 인간 도파민 신경세포의 대량 생산을 가능하게 하였다. 그러나, 장기간 계대 배양한 인간 배아줄기세포 유래 신경전구세포의 생존은 시험관 내 및 세포 이식 후 생체 내(*in vivo*)에서 급격하게 감소하였다. 본 연구에서 이러한 세포 생존의 문제는 Bcl-XL 와 sonic hedgehog 의 외부 유전자를 도입함으로써 해결되었을지라도, 세포 생존 문제는 앞으로 더 연구해야 할 과제로 남아 있다.

핵심되는 말 : 인간 배아줄기세포, 신경전구세포, 도파민 신경세포, 파킨슨병, Bcl-XL, sonic hedgehog